JOURNAL OF GEOPHYSICAL RESEARCH, VOL. 111, B11207, doi:10.1029/2006JB004327, 2006

Stability of arc lower crust: Insights from the Talkeetna arc section, south central Alaska, and the seismic structure of modern arcs

Mark D. Behn[1] and Peter B. Kelemen[2]

Received 4 February 2006; revised 13 June 2006; accepted 2 August 2006; published 11 November 2006.

[1] One process for the formation of continental crust is the accretion of arc terranes at continental margins. A longstanding problem with this model is that although the composition of the continental crust is andesitic, the majority of arc lavas are basaltic. Moreover, those arc lavas that are andesitic tend to be evolved (lower Mg #) compared to the continental crust. Continental crust can be produced through mixing of basaltic and silicic arc lava compositions, assuming that mafic cumulates formed during generation of the silicic component are removed. If these cumulates are denser than the underlying mantle, removal can occur via foundering of lower arc crust. Indeed, field observations of the Talkeetna arc section in south central Alaska, combined with modeling of fractionation in primitive arc magmas, suggest that large amounts of primitive gabbronorite and pyroxenite are missing from the lower crust. Using rock compositions from the Talkeetna section and the free energy minimization program Perple_X, we calculated equilibrium mineral assemblages for a range of gabbroic and ultramafic compositions at P, T, oxygen fugacity (fO_2), and H_2O contents appropriate for arc lower crust. The quartz-olivine-garnet-free mineral assemblage found in the Talkeetna gabbronorites (and in the similar Kohistan section in Pakistan) defines a narrow range of fO_2 centered on NNO+2 (±1 log unit). Predicted mineral assemblages calculated under these conditions were used to estimate the density and seismic structure of the arc lower crust. We find that the missing gabbroic and ultramafic rocks from the Talkeetna section were likely denser than the underlying mantle, while the gabbronorites that remain are either neutrally or slightly positively buoyant. Generalizing, we show that lower crustal Vp > 7.4 km/s in modern arcs is indicative of lower crust that is convectively unstable relative to the underlying mantle. However, most lower crust in modern arcs is observed to have Vp < 7.4 km/s, implying that gravitationally unstable material must founder rapidly on geologic timescales, or high Vp plutonic rocks crystallize beneath the Moho.

Citation: Behn, M. D., and P. B. Kelemen (2006), Stability of arc lower crust: Insights from the Talkeetna arc section, south central Alaska, and the seismic structure of modern arcs, *J. Geophys. Res.*, *111*, B11207, doi:10.1029/2006JB004327.

1. Introduction

[2] A fundamental paradox in understanding the formation of the Earth's continents is that although the continental crust has an andesitic bulk composition, the majority of melts derived from the mantle are basaltic. For decades workers have sought to determine by what process and under what conditions these basaltic melts differentiate to form continental crust. Volcanic arcs are often considered a likely source for continental crust due to the presence of high Mg # (Mg/(Mg + Fe)) andesites with similar major and trace element compositions to the continental crust [e.g., *Kelemen et al.*, 2003a, 2003c; *Taylor*, 1967]. However, primitive and high Mg # andesites are rare in modern arcs, so that the majority of erupted arc lavas are basaltic, and most andesitic lavas in arcs are more evolved (lower Mg # at a given SiO_2 content) than continental crust. This is consistent with the fact that experimental and calculated fractionation trends for basaltic parental magmas generally do not produce high Mg # andesites [*Kelemen*, 1995].

[3] One mechanism for forming high Mg # andesites that would circumvent these problems is through the mixing of basaltic and granitic end-members of a fractionation trend derived from parental basaltic magmas [e.g., *Grove et al.*, 1982; *McBirney et al.*, 1987]. For this model to be a viable explanation for the bulk composition of the continental crust, a mechanism is required to remove the mafic cumulates formed during the generation of the granitic end-member. A popular model for this removal process is through the "foundering" of a lower crustal layer enriched in mafic cumulates [*Arndt and Goldstein*, 1989; *DeBari and Sleep*, 1991; *Herzberg et al.*, 1983; *Kay and Kay*, 1988, 1985; *Kelemen et al.*, 2003a; *Turcotte*, 1989]. Several

[1]Department of Geology and Geophysics, Woods Hole Oceanographic Institution, Woods Hole, Massachusetts, USA.
[2]Lamont Doherty Earth Observatory, Columbia University, Palisades, New York, USA.

0148-0227/06/2006JB004327$09.00

studies have quantified this hypothesis, showing that under high-pressure and low-temperature conditions, many mafic lower crustal compositions will produce a high-density mineral assemblage (dominated by the formation of garnet and/or relatively Fe-rich pyroxene) that is denser than the underlying mantle [*Jull and Kelemen*, 2001; *Müntener et al.*, 2001]. This can produce a lower crustal layer that is gravitationally unstable and sinks back into the mantle [*Kay and Kay*, 1991, 1993]. *Jull and Kelemen* [2001] found that end-member primitive gabbronorite and cumulate ultramafic compositions, under P,T conditions appropriate for arc lower crust (800°C–1000°C at 1 GPa), are likely to be gravitationally unstable. Moreover, given the low viscosity of crustal mineral assemblages at temperatures above 800°C, *Jull and Kelemen* [2001] calculated instability times of only 10^4–10^6 years.

[4] Evidence for lower crustal foundering has been derived from lower crustal xenoliths, seismic imaging, and observed uplift patterns [e.g., *Ducea and Saleeby*, 1996, 1998; *Lee et al.*, 2000; *Saleeby et al.*, 2003; *Zandt et al.*, 2004]. More recently, direct observation of the Jurassic Talkeetna arc section in south central Alaska, combined with fractionation modeling of primitive arc magmas in this section, have provided addition evidence. On the basis of modeling the liquid line of descent in the arc lavas, *Greene et al.* [2006] predicted that large proportions of primitive gabbronorite and pyroxenite should be present in the lower crust. Similarly, *Kelemen et al.* [2003a] showed that the Talkeetna liquid line of descent in particular, and arc fractionation in general, should result in formation of about 30 wt % cumulates with Mg # between ~90 and 83. Yet few gabbronorites with Mg # > 83, and only a thin (~500 m thick) layer of pyroxenite (Mg # 83–91) are observed in the field [*Burns*, 1985; *DeBari and Coleman*, 1989; *DeBari and Sleep*, 1991; *Kelemen et al.*, 2003a], suggesting that a significant component of the lower crust has been removed. Similarly, compositions of lower crustal rocks in the Kohistan arc section (Pakistan Himalaya) compiled by *Kelemen et al.* [2003a] include no primitive gabbros with Mg # > 80, and there is only a thin layer of ultramafic rocks immediately above the Moho.

[5] While these observations support the foundering hypothesis, it is uncertain how representative obducted arc sections are of both the original arc crust and modern volcanic arcs. Furthermore, although *Jull and Kelemen* [2001] examined the stability of a few end-member lower crustal compositions, they did not investigate stability over the range of compositions observed in the Talkeetna and Kohistan sections, nor did they assess the influence of hydrous mineral phases on lower crustal density. It might be possible that the presence of hydrous phases could reduce bulk crustal density and stabilize the lower crust, as pyroxene is replaced by lower density amphibole. Finally, *Jull and Kelemen* [2001] did not estimate seismic velocities for the lower crust, and so were not able to compare the density structure of the Talkeetna and Kohistan sections to modern volcanic arcs.

[6] In this study, we combine field observations, thermodynamic modeling, and seismic data to constrain the conditions of igneous crystallization in arc lower crust and to determine whether lower crustal foundering is a likely, ongoing process in modern arcs. Using the Talkeetna arc section as a compositional model, we calculate crystallizing mineral assemblages for a range of gabbroic and ultramafic compositions at pressure, temperature, oxygen fugacity (fO_2), and H_2O contents appropriate for arc lower crust. The predicted mineral assemblages are used to calculate density and seismic structure for lower arc crust. We find that the missing gabbroic and ultramafic rocks from the Talkeetna section were likely denser than the underlying mantle, while the remaining gabbronorites are neutrally or slightly positively buoyant. In addition, we show that arc lower crustal rock compositions that are denser than the underlying mantle generally have P wave velocities > 7.4 km/s. Because the lower crust in most modern arcs is characterized by P wave velocities < 7.4 km/s, we hypothesize that either gravitationally unstable material never forms, founders rapidly on geologic timescales, or crystallizes beneath the Moho in modern arcs.

2. Thermodynamic Modeling of Arc Lower Crust

[7] In order to estimate the density and seismic P and S wave velocity of arc lower crust it is necessary to determine what mineral phases are present. To first order, these mineral assemblages can be estimated from exposures of lower crustal rocks at the Earth's surface and the elastic properties of these rocks and their component minerals can then be measured in the laboratory at pressures appropriate for the lower crust [e.g., *Birch*, 1960, 1961; *Christensen and Fountain*, 1975; *Miller and Christensen*, 1994]. However, there are several disadvantages to this method. First, few laboratory studies have measured physical properties of crustal rocks at the high temperatures appropriate for arc lower crust. Thus reequilibration does not occur during the experiments and the measured elastic properties reflect the mineral assemblage present at the sample's final equilibration conditions rather than the in situ P, T conditions appropriate for the lower crust. Furthermore, individual laboratory measurements are labor intensive and therefore cannot be used to explore a wide range of compositional space (e.g., major element composition, H_2O content, oxidation state). Finally, the laboratory measurements do not allow direct prediction of the mineral assemblage, density and seismic velocity of the same rock composition at a different pressure and temperature.

[8] An alternative approach for estimating the elastic properties of lower crustal rocks is to use thermodynamic modeling to calculate the equilibrium mineral assemblage for a given bulk composition at specific P, T conditions [e.g., *Sobolev and Babeyko*, 1994]. Density and seismic velocity can then be estimated from mixing theory using experimental data on pure mineral phases [e.g., *Watt et al.*, 1976]. Because of the computationally efficiency of this method a broad compositional space can be easily searched. Calculations of density and seismic velocity made in this fashion require accurate knowledge of the elastic properties of pure mineral phases and their pressure and temperature derivatives. For these data, we utilize a recent compilation of physical properties for crustal and upper mantle minerals by *Hacker et al.* [2003].

[9] This computational approach has been used by several investigators to estimate the density and seismic struc-

Table 1. Average Lower Crustal and Upper Mantle Compositions

	SiO_2	TiO_2	Al_2O_3	FeO*	MnO	MgO	CaO	Na_2O	K_2O	Mg#
Crustal compositions										
Talkeetna Gabbronorite[a]	47.86	0.66	19.00	9.94	0.18	7.78	12.53	1.82	0.16	58.3
Tonsina Gabbronorite[b]	45.66	0.86	19.26	11.53	—	7.69	12.88	1.74	0.07	54.3
Tonsina Pyroxenite[a]	49.95	0.07	3.42	8.31	0.17	27.95	9.88	0.22	0.02	85.7
Mantle compositions										
Talkeetna Harzburgite[a]	44.63	0.01	0.60	7.91	0.13	46.00	0.54	0.15	0.01	91.2
Pyrolite[c]	45.10	0.20	3.30	8.00	0.15	38.10	3.10	0.40	0.03	89.5

[a]*Kelemen et al.* [2003a].
[b]*Burns* [1983].
[c]*Ringwood* [1979].

ture of the lower continental crust [*Behn and Kelemen*, 2003; *Hacker et al.*, 2003; *Jull and Kelemen*, 2001; *Sobolev and Babeyko*, 1994]. The applicability of these studies to arc lower crust is limited by several simplifying assumptions that were incorporated in the thermodynamic calculations. For example, amphibolite to granulite facies arc lower crust can contain up to 2 wt % H_2O in hydrous minerals, which may significantly decrease the density and seismic velocity of the lower crust. Yet, with the exception of *Hacker et al.* [2003], previous studies assumed anhydrous equilibration conditions for the crust. Moreover, *Hacker et al.* [2003] examined only end-member water-saturated mid-ocean ridge basalt (MORB) and ultramafic compositions and did not explore the influence of intermediate water contents or variations in major element composition on the density and seismic velocity of the lower crust. Finally, none of these studies investigated the influence of oxidation state on the equilibrating phase assemblages and the physical properties of arc lower crust. This is particularly relevant for volcanic arcs, where erupted lavas are observed to be significantly more oxidized than normal mid-ocean ridge basalts [e.g., *Carmichael*, 1991].

[10] In this study we address these issues by performing a series of thermodynamic calculations optimized for the conditions found in the lower crust of active arcs in order to assess the potential for lower crustal foundering and to quantify the compositional implications for the seismic structure of arc lower crust. As a compositional model for arc crust we choose the Talkeetna section exposed in south central Alaska. The Talkeetna section represents a well-preserved fragment of an island arc that was active from 175 to 200 Ma [e.g., *Plafker et al.*, 1989; M. Rioux et al., The magmatic development of an intra-oceanic arc: High-precision U-Pb zircon and whole-rock isotopic analyses from the accreted Talkeetna arc, south-central Alaska, submitted to *Geological Society of America Bulletin*, 2006]. The crust-mantle transition is exposed in the Tonsina area where it extends laterally over several kilometers [*DeBari and Coleman*, 1989]. The lower Talkeetna crust is composed primarily of gabbronorite with a relatively homogeneous major element composition [*Burns*, 1985; *DeBari and Coleman*, 1989; *DeBari and Sleep*, 1991; *Greene et al.*, 2006; *Kelemen et al.*, 2003a]. These gabbronorites overlie a thin (~500 m) pyroxenite layer, which in turn overlies residual mantle harzburgite. Table 1 lists the average bulk composition used for each of these layers in our modeling. We note that the average Talkeetna gabbronorite bulk composition of *Kelemen et al.* [2003a] is characterized by higher Mg # and higher SiO_2 content than that reported by *Burns* [1983] for gabbronorites in the Tonsina area. This difference is likely due to the incorporation of many relatively high Mg # gabbros from the deeper parts of the Talkeetna section in the average of *Kelemen et al.* [2003a], whereas *Burns* [1983] concentrated on samples from midcrustal exposures near the plutonic/volcanic contact.

2.1. Calculation of Subsolidus Phase Equilibria

[11] Subsolidus phase equilibrium calculations were performed using the free energy minimization algorithm Perple_X [*Connolly*, 1990, 2005] and the thermodynamic database of *Holland and Powell* [1998]. Calculations were performed for initial bulk compositions that include the major element oxides SiO_2, Al_2O_3, FeO*, MgO, CaO, Na_2O, and a range of H_2O contents from 0–0.5 wt %. TiO_2, K_2O, and P_2O_5 were excluded for simplicity, as they do not significantly affect the calculated subsolidus modes, but do require addition of many, poorly characterized solid solution models to the free energy minimization calculations. The H_2O contents used in our calculations are based

Table 2. Solid Solution Models and Data Sources[a]

Phase	Formula	Source[b]
Olivine[c]	$Mg_{2x}Fe_{2y}Mn_{2(1-x-y)}SiO_4$, $x + y \leq 1$	HP98
Orthopyroxene	$Mg_{x(2-y)}Fe_{(1-x)(2-y)}Al_{2y}Si_{2-y}O_6$	HP96
Clinopyroxene	$Na_{1-y}Ca_yMg_{xy}Fe_{(1-x)y}Al_ySi_2O_6$	HP96
Plagioclase	$Na_xCa_{1-x}Al_{2-x}Si_{2+x}O_8$	NCK80
Spinel	$Mg_xFe_{1-x}Al_2O_3$	HP98
Garnet[c]	$Fe_{3x}Ca_{3y}Mg_{3z}Mn_{3(1-x-y-z)}Al_2Si_3O_{12}$, $x + y + z \leq 1$	HP98
Amphibole	$Ca_{2-2w}Na_{z+2w}Mg_{(3+2y+z)x}Fe_{(3+2y+z)(1-x)}Al_{3-3y-w}Si_{7+w+y}\ O_{22}(OH)_2$, $w + y + z \leq 1$	WP03, WPH03
Melt	Na-Mg-Al-Si-K-Ca-Fe hydrous silicate melt	HP01, WPH01

[a]Compositional variables w, x, y, and z vary between 0 and 1 and are calculated as a function of temperature and pressure using the free energy minimization algorithm Perple_X'04 [*Connolly*, 1990, 2005]. See Perple_X documentation for further details. Sources are HP96 [*Holland and Powell*, 1996]; HP98 [*Holland and Powell*, 1998]; HP01 [*Holland and Powell*, 2001]; NCK80 [*Newton et al.*, 1980]; WP03 [*Wei and Powell*, 2003]; WPH01 [*White et al.*, 2001]; WPH03 [*White et al.*, 2003].
[b]Wherever possible, the Holland and Powell solution models have been chosen for internal consistency.
[c]Because Mn was not included in the bulk compositions the Mn component is set to zero in all calculations.

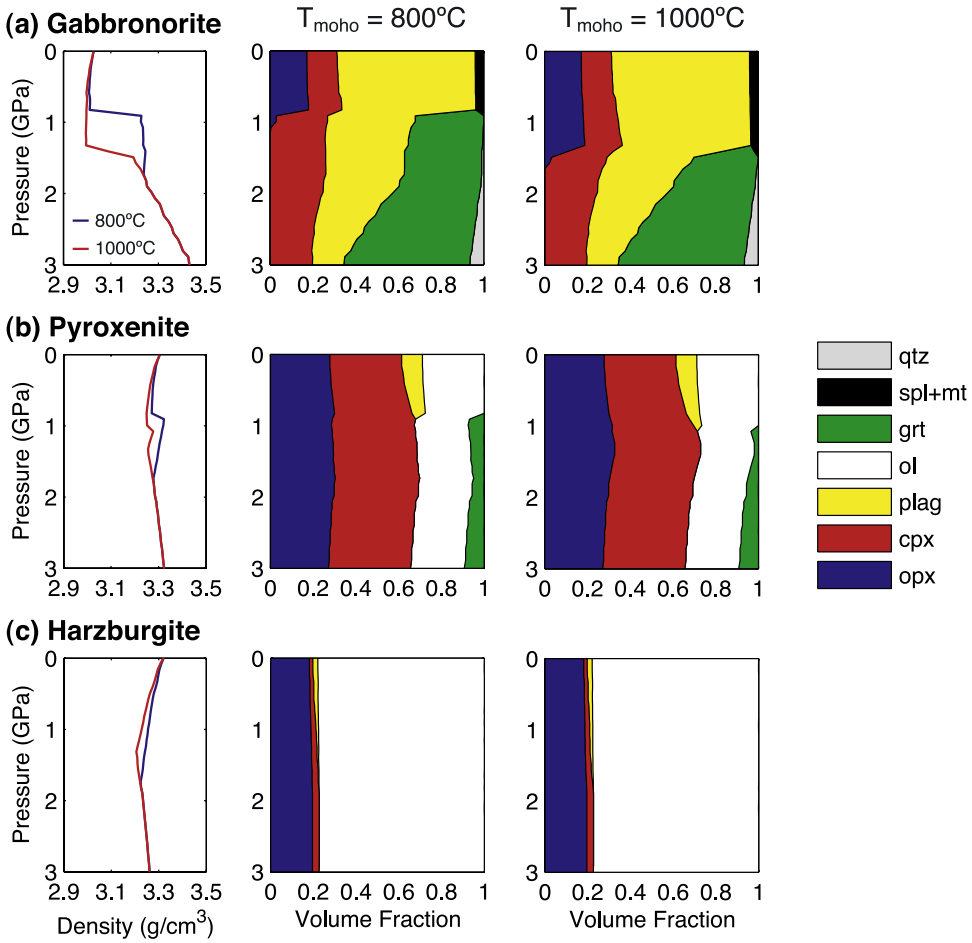

Figure 1. Calculated equilibrium mineral assemblages and corresponding density profiles for the average (a) Talkeetna gabbronorite, (b) Tonsina pyroxenite, and (c) Talkeetna harzburgite compositions (see Table 1). Densities and modes are calculated along end-member arc geotherms, which reach 800°C and 1000°C at 1 GPa, respectively, and are adiabatic for pressures greater than 1.75 GPa. An oxygen fugacity of NNO+2 is assumed for the gabbronorite and pyroxenite calculations, and an FMQ buffer is used for the harzburgite. Mineral abbreviations are (qtz) quartz, (spl + mt) spinel + magnetite, (grt) garnet, (ol) olivine, (plag) plagioclase, (cpx) clinopyroxene, and (opx) orthopyroxene (see Table 2 for solution models used).

on observed hornblende modes ranging from 5–20 vol % in gabbronorites from the Talkeetna arc section [*Greene et al.*, 2006]. Solid solutions were assumed for olivine, clinopyroxene, orthopyroxene, plagioclase, garnet, spinel, and amphibole (see Table 2 for solution models and references). Wherever possible the Holland and Powell solution models were used for internal consistency. We note that Perple_X does not incorporate CaTs, MgTs, and/or FeTs in the pyroxene solution models. The result is that we tend to slightly over predict spinel + clinopyroxene and/or plagioclase + olivine in our calculations. While this has the potential to raise problems at high temperatures it is unlikely to have a significant effect at the low temperatures involved in this study. The oxidation state of the system in the calculations was controlled using pressure and temperature-dependent fO_2 buffers ranging from fayalite-magnetite-quartz (FMQ) to hematite-magnetite (HM).

[12] For each bulk composition, the crystallizing mineral assemblages are determined along two end-member arc geotherms defined to have Moho temperatures of 800°C and 1000°C, respectively, at 1 GPa. These end-member geotherms are based on petrological constraints of crustal P-T conditions from the Talkeetna and Kohistan arc sections [*DeBari and Coleman*, 1989; *Kelemen et al.*, 2003b]. For temperatures <800°C mineral modes and compositions were frozen. This minimum equilibration temperature represents a likely lower bound on net transfer reactions (nucleation and growth of new mineral phases) during cooling and/or decompression under anhydrous lower crustal conditions [*Austrheim*, 1998; *Hacker et al.*, 2000]. In section 4.3 we explore the influence of lower minimum equilibration temperatures, which may be more appropriate for the hydrous conditions found in some arc crust.

2.2. Calculation of Density, Vp, and Vs for Mineral Aggregates

[13] The calculated mineral assemblages are used to determine density, Vp, and Vs at each point along the geotherm. The elastic properties of the multiphase assemblages are estimated at elevated pressure and temperature

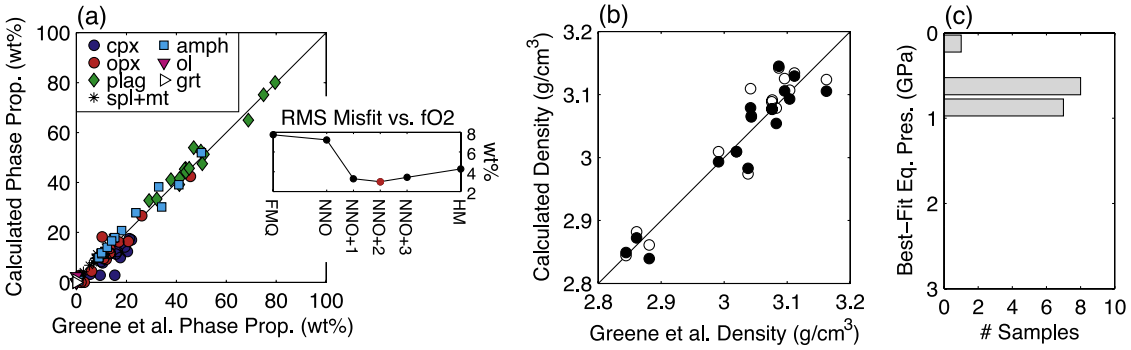

Figure 2. (a) Comparison of calculated equilibrium phase assemblages with phase proportions determined by mass balance for 16 Talkeetna gabbronorite samples [*Greene et al.*, 2006]. The best fit phase assemblages are determined for calculations along an 800°C geotherm. Inset shows the sum-of-squares misfit as a function of the oxygen fugacity buffer. The minimum misfit is found for NNO+2 (shown). (b) Comparison of densities calculated from equilibrium mineral modes assuming NNO (open) and NNO+2 (solid) buffers to densities calculated from *Greene et al.* [2006] modes. (c) Histogram illustrating the best fit equilibrium pressure. All but one sample is predicted to crystallize at pressures appropriate for the midcrust to lower crust (0.5–1 GPa).

following the method of *Hacker et al.* [2003]. In this approach, the properties of individual minerals are first corrected for the effects of pressure and temperature. In the case of solid solutions, the solution phases are decomposed into their end-member components and elastic properties are calculated for each end-member. This decomposition is necessary because experimental data on physical properties is typically only available for end-member mineral compositions. Once the individual mineral properties have been determined, the properties of the aggregate mineral assemblage are estimated using the average of the Hashin-Strikman bounds. We note that these calculations assume zero residual porosity, which is likely a valid assumption for pressures exceeding 0.2–0.3 GPa [*Behn and Kelemen*, 2003, Figure 6].

[14] Figure 1 illustrates calculations for the average gabbronorite, pyroxenite and harzburgite compositions (Table 1) along 800°C and 1000°C geotherms. The variations in density for the gabbronorite composition are dominated by changes in the phase assemblage (Figure 1a). In particular, the large increase in density at ~0.85 GPa corresponds to formation of garnet associated with reactions such as anorthite + enstatite = garnet + qtz and $CaAl_2SiO_6$ (Calcium Tschermak's molecule in pyroxene) + enstatite = garnet.

[15] The pyroxenite composition also displays a step in density around 0.8 GPa (Figure 1b). At pressures <0.8 GPa, Perple_X predicts a small amount of plagioclase in the pyroxenite, which is replaced by garnet at pressures >0.8 GPa. In calculations on a different pyroxenite bulk composition, *Jull and Kelemen* [2001] showed that plagioclase reacted to form a spinel pyroxenite assemblage at relatively low pressure, and then garnet pyroxenite at higher pressure. In both sets of calculations, the loss of plagioclase from the phase assemblage yields a pyroxenite that is 50 to 70 kg/m^3 denser than residual peridotite, as predicted in general for pyroxenites by *Arndt and Goldstein* [1989]. It is significant that the loss of plagioclase, rather than the presence of garnet versus spinel, is the main cause of the density increase with increasing pressure in the pyroxenite bulk compositions. The reason for this is that garnet is not found in Talkeetna pyroxenites near the Moho, where samples yield an equilibration pressure of about 1 GPa, while spinel-rich pyroxenites are abundant [*DeBari and Coleman*, 1989; *Kelemen et al.*, 2003a].

[16] Finally, in contrast to the gabbronorite and pyroxenite, the phase assemblage for harzburgite remains relatively constant with depth and the gradual variations in harzburgite density are caused by changes in mineral compressibility along the geotherm (Figure 1c).

3. Conditions of Igneous Crystallization in Arc Lower Crust

[17] Before examining the physical properties of the Talkeetna lower crust, it is necessary to ensure that our computational approach accurately approximates the true mineral assemblages. To address this issue we calculated mineral assemblages for a suite of 16 gabbronorites from the Talkeetna section for which modes have been determined by mass balance of the whole rock and mineral chemistry [*Greene et al.*, 2006]. For each sample we calculated the crystallizing mineral assemblages along an 800°C geotherm over a range of fO_2 buffers. The water content of each sample is estimated based on the *Greene et al.* [2006] amphibole mode assuming 2.5 wt % H_2O in hornblende. Texturally, the hornblende in most gabbronorites is interstitial and/or rimming pyroxenes. The compositions of the hornblendes [*Greene et al.*, 2006] suggest to us that it is a late stage igneous phase in these rocks.

[18] In Figure 2 we compare our calculated modes along the 800°C geotherm to the *Greene et al.* [2006] mass balanced modes and determine the P, T conditions that result in the best fitting mineral assemblage. The sum-of-the-squares misfit for all samples is then evaluated as a function of oxygen fugacity. We find that the *Greene et al.* [2006] modes are best fit by mineral assemblages calculated on fO_2 buffers between NNO+1 and NNO+3 (Figure 2a) and pressures of 7–10 kbar (Figure 2c), consistent with crystallization in the lower crust at depths of 25–35 km. The *Greene et al.* [2006] mineral modes can be equally well fit along a 1000°C geotherm, but with best fitting equili-

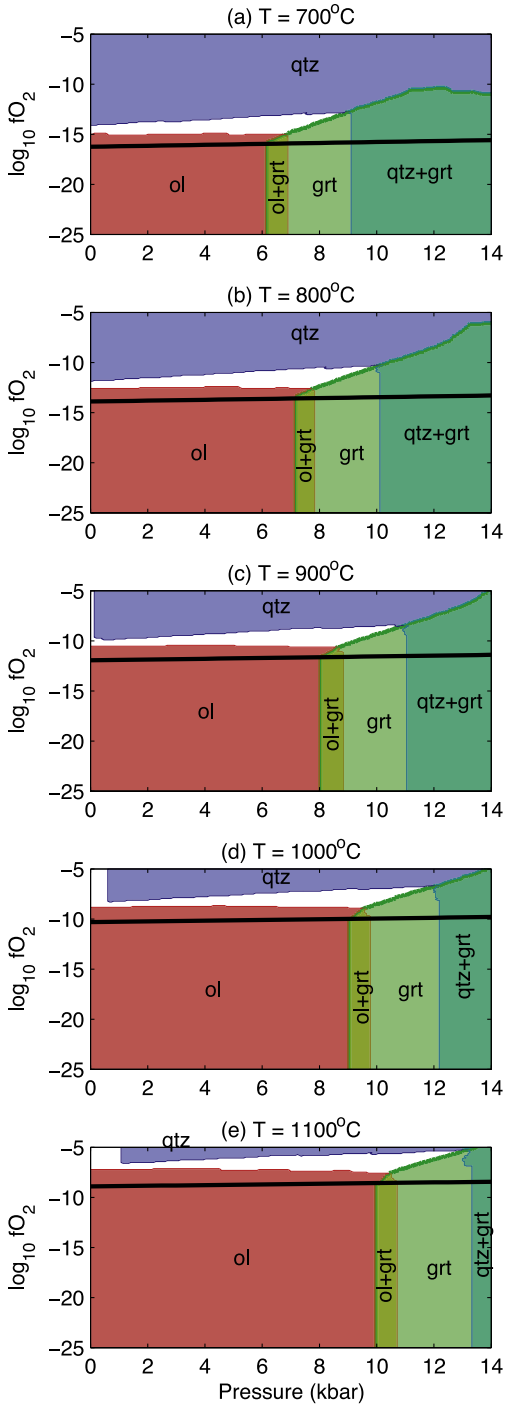

Figure 3. Calculations showing the stability field of olivine (red), garnet (green), and quartz (blue) as a function of pressure and fO_2 for the average Talkeetna gabbronorite composition. Calculations are performed at temperatures of (a–e) 700°C–1100°. The thick black line illustrates the position of the NNO buffer for fO_2. Field observations show Talkeetna gabbronorites to lack olivine, quartz, and garnet, limiting their crystallization conditions to a narrow range of fO_2 corresponding to an NNO+2 buffer (white region).

bration pressures that are ~0.25 kbar higher than for the 800°C geotherm.

[19] The sensitivity of the calculated misfit to oxygen fugacity is mainly due to suppression of olivine in favor of orthopyroxene + clinopyroxene + magnetite at high fO_2 and suppression of quartz in favor of orthopyroxene + magnetite at low fO_2. Almost all gabbronorites in the Talkeetna section lack quartz, olivine, and garnet [*Greene et al.*, 2006]. Allowing fO_2 to behave as an independent variable, we show that for the average Talkeetna gabbronorite composition this characteristic mineral assemblage defines a narrow range of fO_2 conditions centered on NNO+2 (±1 log unit), with the upper and lower bounds defined by the stability fields of quartz and olivine, respectively (Figure 3). On the basis of these results, we conclude that an NNO+2 buffer is most appropriate for Talkeetna arc lower crust and assume this fO_2 buffer in calculations of phase equilibria for lower crustal rocks throughout the remainder of the study.

[20] For NNO+2 and an 800°C geotherm, the densities calculated from the best fitting mineral modes have an average misfit of 2 kg/m^3 with a standard deviation of 31 kg/m^3 relative to the densities calculated from the *Greene et al.* [2006] mass balance modes (Figure 2b). Unlike the calculated mineral assemblages, which were shown to be highly sensitive to fO_2, the densities are not strongly affected by the oxygen fugacity. For example, while the predicted mineral modes vary dramatically between NNO and NNO+2 (Figure 2a), the average change in density is less than 10 kg/m^3, and the largest change in density for an individual sample is less than 30 kg/m^3 (Figure 2b). The lack of a correlation between fO_2 and density is a result of the similar density of olivine compared to magnetite + orthopyroxene in the same bulk composition. On the basis of these results, we conclude that arc lower crust stability is relatively insensitive to oxidation state.

4. Density Structure and Stability of the Lower Talkeetna Crust

[21] Following the approach outlined above, we quantify the stability of the lower Talkeetna crust by comparing the densities of the average Talkeetna gabbronorite and Tonsina pyroxenite to the density of the underlying harzburgite (Figure 4). For anhydrous crustal and mantle compositions, we find that the average Talkeetna gabbronorite is nearly neutrally buoyant between pressures of 0.9–1.8 GPa on an 800°C geotherm, becoming unstable (i.e., $\rho_{gabbro} > \rho_{harz}$) only at pressures greater than 1.9 GPa (well below the base of typical arc crust). In contrast, the average Tonsina gabbronorite reported by *Burns* [1983] produces a higher density mineral assemblage, owing to its lower Si and higher Fe content, and is denser than underlying mantle peridotite at all pressures greater than ~0.9 GPa. The Tonsina pyroxenite is unstable at all pressures greater than ~0.8 GPa, with a relatively modest density contrast of ~70 kg/m^3. However, *Jull and Kelemen* [2001] showed that such a density contrast is sufficient to drive convective instability on timescales of ~10 million years or less. For all three compositions, the abrupt increase in density near 0.8 GPa is associated with the decrease in the proportion of plagioclase, and the resulting formation of garnet in some rocks (Figure 1). Below we investigate the sensitivity of lower crustal densities to Moho

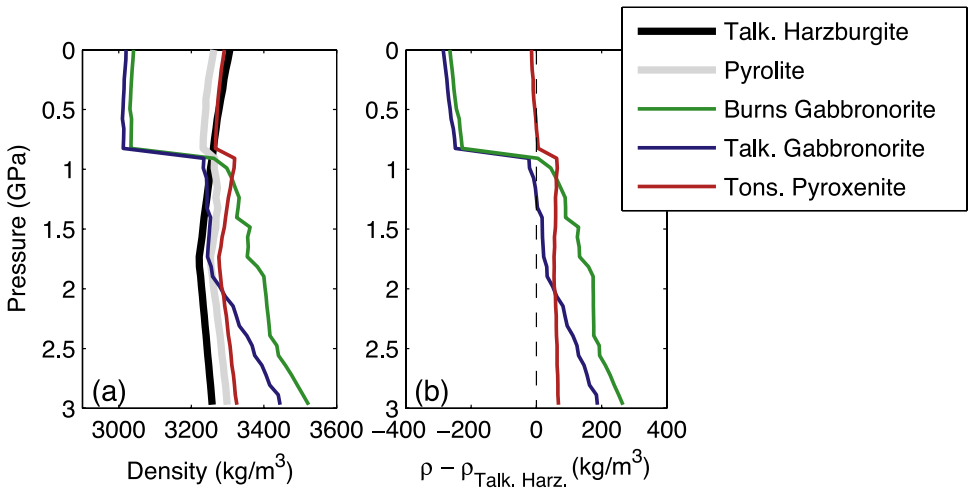

Figure 4. (a) Comparison of density as a function of pressure for average Talkeetna lower crustal and mantle compositions (Table 1) along an 800°C geotherm. Calculations for crust and mantle compositions are performed along NNO+2 and FMQ buffers, respectively. (b) Density contrast between crustal compositions and average Talkeetna harzburgite. Note that the *Burns* [1983] gabbronorite and Tonsina pyroxenite are both unstable at 1 GPa, while the average Talkeetna gabbronorite is neutrally or slightly positively buoyant.

temperature, water content, minimum equilibration temperature, and major element chemistry.

4.1. Spinel Versus Garnet Pyroxenite

[22] Our calculations produce garnet at the expense of plagioclase, even in the pyroxenite bulk composition. However, garnet is not present in Talkeetna pyroxenites that equilibrated at about 1 GPa. For this reason, here we go into some detail in considering the relative density of garnet and spinel pyroxenites versus residual peridotites. In olivine- and quartz-free pyroxenites, any calcic plagioclase present at low pressure is consumed as a result of increasing pressure via reactions such as

$$\underset{\text{Anorthite (plag)}}{CaAl_2Si_2O_8} + \underset{\text{Spinel}}{MgAl_2O_4} + \underset{\text{Enstatite (pyroxene)}}{Mg_2Si_2O_6} = \underset{\text{MgTschermak's (pyroxene)}}{2MgAl_2SiO_6} + \underset{\text{Diopside (pyroxene)}}{CaMgSi_2O_6} \quad \text{(R1)}$$

and

$$\underset{\text{Anorthite (plag)}}{CaAl_2Si_2O_8} + \underset{\text{Spinel}}{MgAl_2O_4} + \underset{\text{Enstatite (pyroxene)}}{Mg_2Si_2O_6} = \underset{\text{garnet}}{CaMg_2Al_2Si_3O_{12}} + \underset{\text{MgTschermak's (pyroxene)}}{MgAl_2SiO_6}, \quad \text{(R2)}$$

similar reactions involving reduction of ferric iron in spinel such as

$$\underset{\text{Anorthite (plag)}}{6CaAl_2Si_2O_8} + \underset{\text{Ferrosilite (pyroxene)}}{3Fe_2Si_2O_6} + \underset{\text{Magnetite}}{2Fe_3O_4} = \underset{\text{FeTschermak's (pyroxene)}}{6FeAl_2SiO_6} + \underset{\text{Hedenbergite (pyroxene)}}{6CaFeSi_2O_6} + O_2 \quad \text{(R3)}$$

and

$$\underset{\text{Anorthite (plag)}}{6CaAl_2Si_2O_8} + \underset{\text{Ferrosilite (pyroxene)}}{3Fe_2Si_2O_6} + \underset{\text{Magnetite}}{2Fe_3O_4} = \underset{\text{garnet}}{6CaFe_2Al_2Si_3O_{12}} + \underset{\text{Oxygen}}{2O_2}, \quad \text{(R4)}$$

and reactions incorporating ferric iron in garnet such as

$$\underset{\text{Anorthite (plag)}}{CaAl_2Si_2O_8} + \underset{\text{Ferrosilite (pyroxene)}}{2Fe_2Si_2O_6} + \underset{\text{Magnetite}}{Fe_3O_4} = \underset{\text{garnet}}{CaFe_5Al_2Fe^{3+}{}_2Si_6O_{24}}. \quad \text{(R5)}$$

[23] Reactions (R1) and (R3) produce a plagioclase- and garnet-free pyroxenite composition, as observed in the Talkeetna pyroxenites. Since Perple_X does not use a spinel solid solution model that incorporates chromium, for Cr-rich ultramafic bulk compositions Perple_X systematically underpredicts the stability of spinel-bearing ultramafic assemblages with respect to garnet-bearing assemblages at moderate pressure (see *Kelly et al.* [2003] and *Jull and Kelemen* [2001] for further discussion). However, as noted by *Arndt and Goldstein* [1989], because the Mg # of igneous pyroxenites is less than that of residual peridotites, while olivine and pyroxene have similar densities at a given Mg #, plagioclase-free pyroxenites with a relatively low Mg # are denser than residual peridotites with a higher Mg #. Thus all of these reactions will produce plagioclase-free pyroxenite assemblages that are denser than residual peridotite, whether garnet is a product or not. This is apparent in Figures 5a–5c, illustrating calculated phase assemblages and densities of the pyroxenite composition compared to residual peridotite. Even with no garnet present, the pyroxenite is predicted to be denser than residual peridotite when the proportion of plagioclase is less than 6–8%.

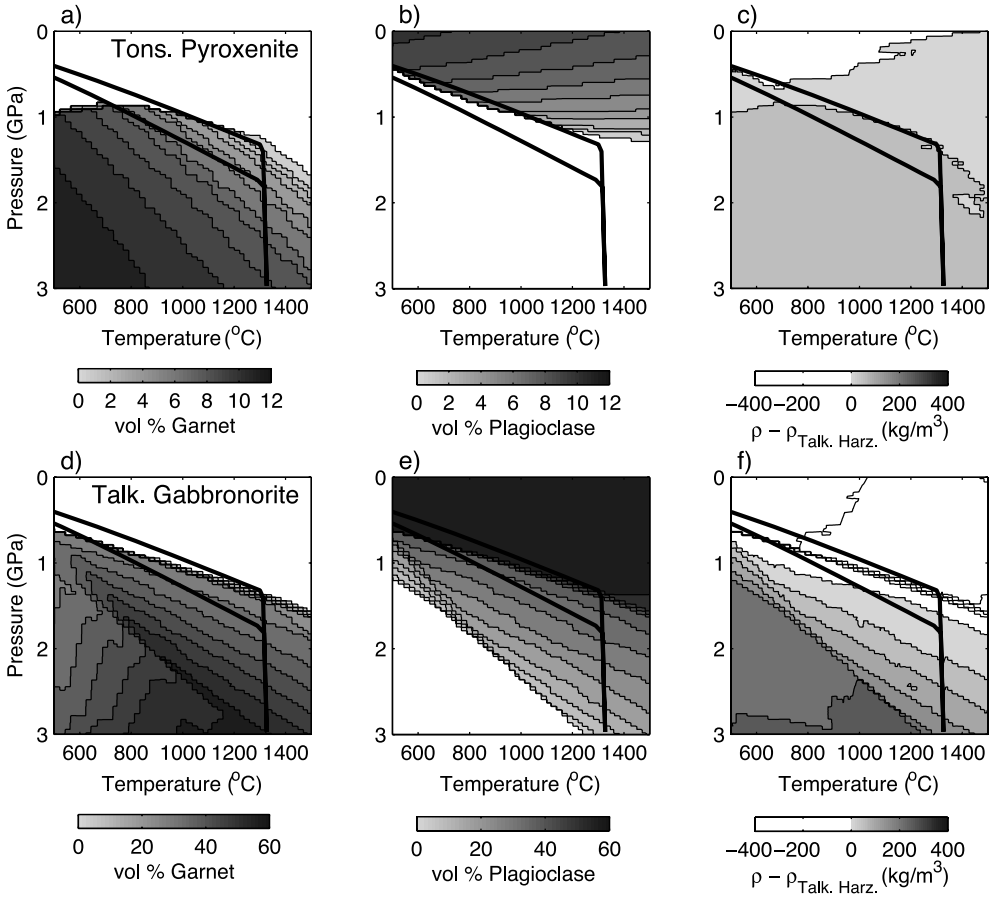

Figure 5. Garnet and plagioclase stability fields and the difference in crustal density relative to harzburgite for the average (a–c) Tonsina pyroxenite and (d–f) Talkeetna gabbronorite compositions, respectively. Thick black lines illustrate the 800°C and 1000°C arc geotherms. The density difference between gabbronorite and harzburgite is dominantly controlled by the garnet mode. In contrast, the pyroxenite is denser than harzburgite even with no garnet present when the plagioclase mode is less than 6–8%.

4.2. Moho Temperature

[24] Estimates based on metamorphic phase equilibria indicate that the base of the Talkeetna crust was probably between 800°C and 1000°C at 1–1.2 GPa [*DeBari and Coleman*, 1989; *Kelemen et al.*, 2003b]. At these pressures, the slope of the garnet-in reaction for both the Talkeetna and Tonsina gabbronorites is nearly parallel to likely arc geotherms (Figure 5d), making the stability of garnet highly sensitive to small changes in temperature. For example, a shift from 1000°C to 800°C at 1 GPa will result in a density increase of more than 250 kg/m^3, due to the formation of garnet at lower temperature (Figures 5f and 6).

[25] In contrast, the plagioclase-out reaction for the Tonsina pyroxenite occurs at lower pressure, and plagioclase-free pyroxenites are denser than residual peridotite whether they include garnet or not, making the density contrast between pyroxenite and residual peridotite at arc Moho conditions less sensitive to temperature (Figure 5). Consequently, while the pyroxenite remains negatively buoyant at 1000°C and 1 GPa, the gabbronorite will be positively buoyant at these higher temperatures (Figure 6).

4.3. Water Content of the Lower Crust

[26] The amphibole modes in the gabbronorites described by *Greene et al.* [2006] imply water contents $\leq$0.5 wt % H_2O in the Talkeetna lower crust. To quantify the influence of a hydrated lower crust on the density of the gabbronorite and pyroxenite, we calculated density for each average composition assuming 0.2 and 0.5 wt % H_2O (Figure 6). For an 800°C geotherm, the presence of H_2O has the largest effect on the gabbronorite density structure between 0.8–1.2 GPa. In this pressure range amphibole replaces plagioclase + pyroxene + garnet resulting in a net reduction of the bulk density by 25–100 kg/m^3. At pressures less than 0.8 GPa, the bulk density also decreases but the magnitude of the change is smaller because garnet is no longer stable and amphibole replaces only pyroxene + plagioclase. Similarly, the substitution of amphibole for pyroxene results in a 10–50 kg/m^3 decrease in pyroxenite density at pressures less than $\sim$1.2 GPa. For pressures exceeding 1.2 GPa along likely arc geotherms (with corresponding temperature greater than 960°C and 1200°C along the 800°C and 1000°C geotherms, respectively), hornblende is not stable and H_2O is predicted to be a free phase. Thus, in the results presented in the Figure 6, H_2O does not affect the bulk (solid) density of either the gabbronorite or the pyroxenite.

[27] The solubility of water in minerals is limited at high temperatures, especially at low pressure. This effect has a strong influence on the density of the hydrated pyroxenite near 1 GPa. Specifically at 1000°C and 1 GPa, hornblende

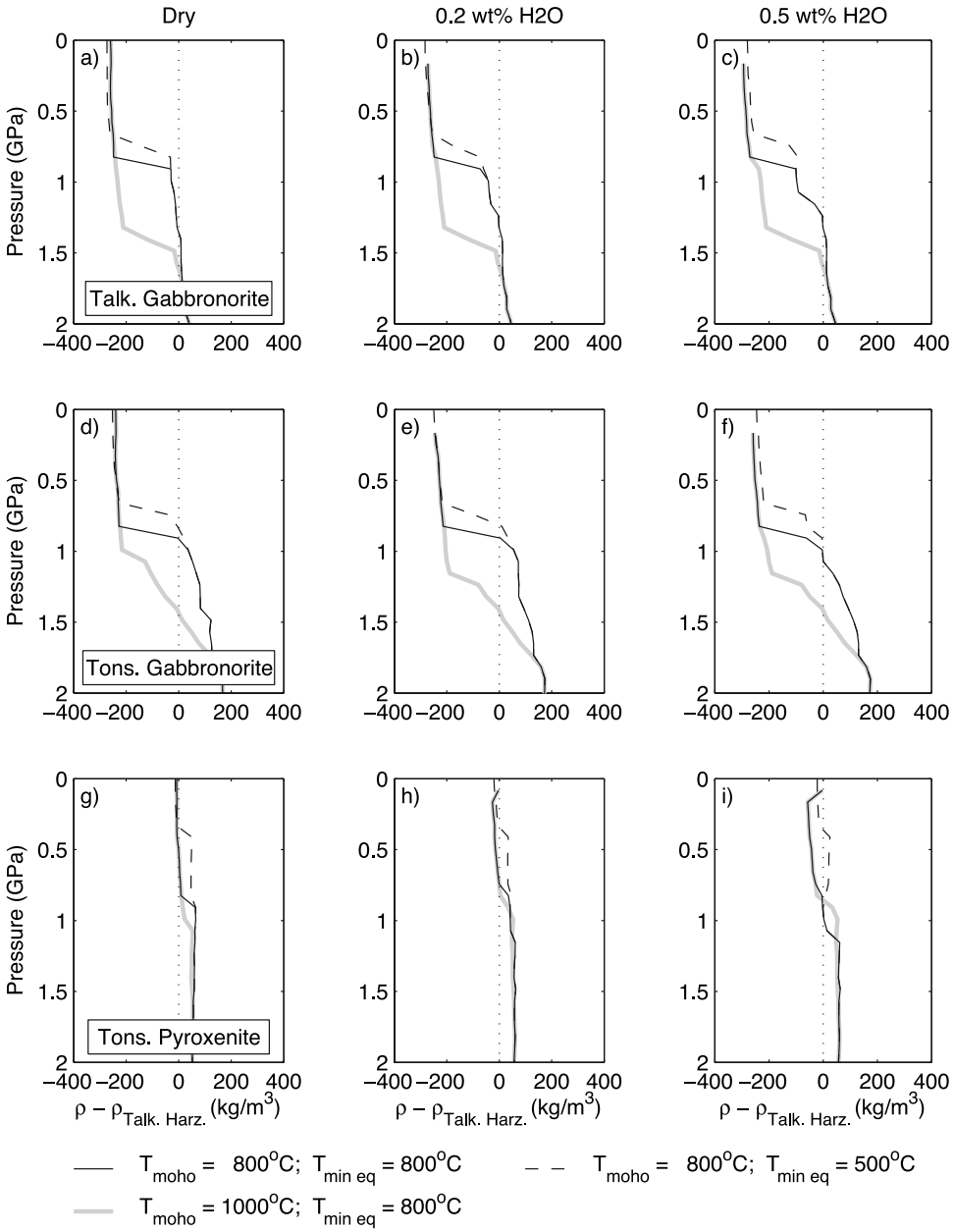

Figure 6. Summary of the influence of Moho temperature, water content, and minimum equilibration temperature on the density contrast between the Talkeetna harzburgite and the (a–c) Talkeetna gabbronorite, (d–f) *Burns* [1983] Tonsina gabbronorite, and (g–i) Tonsina pyroxenite. Calculations for crust and mantle compositions are performed along an NNO+2 and FMQ buffer, respectively. Increasing water contents of 0, 0.2, and 0.5 wt % H_2O are illustrated in panels from left to right. Solid lines show density contrasts determined with a minimum equilibration temperature of 800°C along 800°C (black) and 1000°C (grey) geotherms. Dashed lines illustrate calculations with a minimum equilibration temperature of 500°C along an 800°C geotherm.

is not predicted to be stable, and H_2O is predicted to be a free phase, resulting in a residual anhydrous mineral assemblage that is denser than the hydrous assemblage predicted for a cooler 800°C geotherm. Thus in a hydrated lower crust, elevated temperatures may result in an increase in crustal density due to the breakdown of hydrous phases.

4.4. Minimum Equilibration Temperature

[28] As discussed earlier, 800°C represents a probable lower bound for retrograde, net transfer reactions in anhydrous rocks at lower crustal conditions. However, under hydrous conditions reaction kinetics are enhanced, and in the Talkeetna arc, significant retrogression occurred down to greenschist-facies conditions. To assess the importance of this effect on lower crustal densities, we performed a series of calculations assuming a minimum equilibration temperature of 500°C (Figure 6). Comparing these results to our earlier calculations with a minimum temperature of 800°C, we find that for the Talkeetna gabbronorite the lower minimum equilibration temperature promotes garnet stabil-

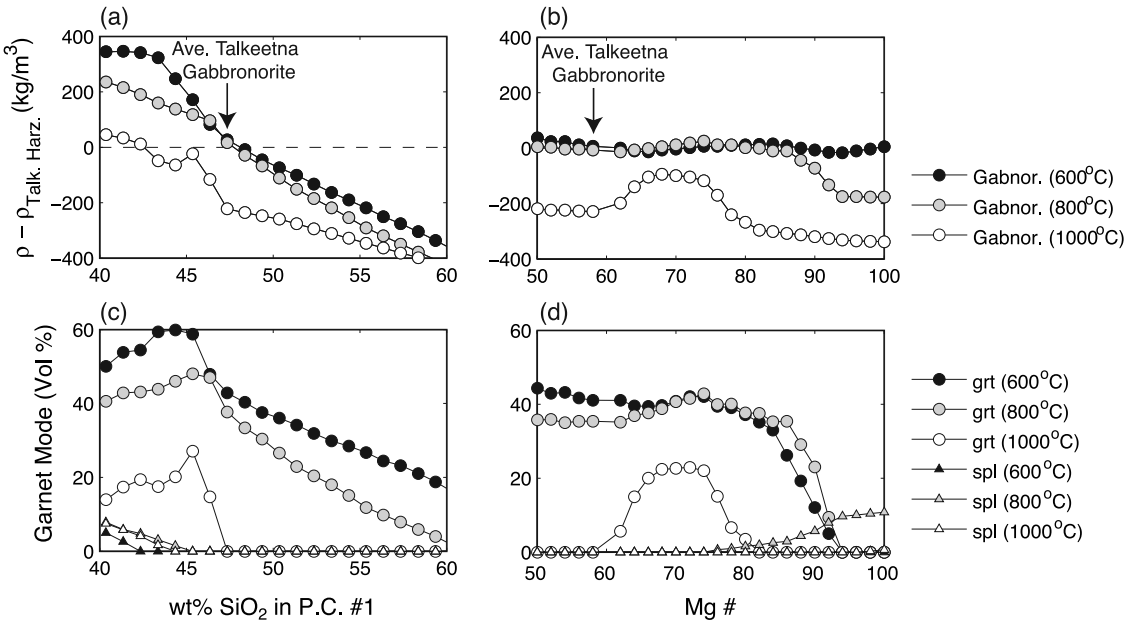

Figure 7. (a, b) Density contrast between crust and mantle and (c, d) garnet and spinel modes as a function of wt % SiO_2 and Mg #, respectively. Synthetic compositions are computed with respect to the average Talkeetna gabbronorite composition (see text for description). In Figure 7a, synthetic compositions lie along the main compositional vector in the Talkeetna gabbronorites, and SiO_2 increase is accompanied by increasing Na_2O and decreasing Al_2O_3, FeO, MgO and CaO. In Figure 7b, variation is only in Mg # and does not affect the relative proportions of oxides other than MgO and FeO. Calculations in are performed at 1 GPa and 600°C (black), 800°C (grey), and 1000°C (open). An NNO+2 buffer is assumed for all calculations. The average Talkeetna gabbronorite is neutrally or slightly positively buoyant, while more primitive compositions with lower SiO_2 and Na_2O are predicted to be gravitationally unstable.

ity at lower pressures. This effect is clearly illustrated by the garnet proportions shown in Figure 5d, in which garnet is stable at 0.7 GPa and 500°C, but not 0.7 GPa and 800°C. The pyroxenite composition is also found to be unstable to lower pressures for a minimum equilibration temperature of 500°C (Figures 6g–6i). In the case of the pyroxenite, the garnet stability field remains relatively unchanged (Figure 5a), but the stability of plagioclase is limited to pressures < 0.4 GPa (Figure 5b), resulting in a predicted increase in density at this pressure. Thus, for both the gabbronorite and pyroxenite compositions the effect of reducing the minimum equilibration temperature is to increase the potential for negatively buoyant mineral assemblages at midcrustal levels or along colder geotherms.

4.5. Major Element Composition

[29] We have shown that the proportion of garnet dominates the stability of the gabbroic lower crustal rocks, and that the small variations in major element chemistry can have a large effect on the predicted crustal densities (e.g., compare the Talkeetna and Tonsina gabbronorites in Figure 4b). Therefore it is important to quantify the influence of major element chemistry on garnet-forming reactions in gabbroic rocks. To characterize the compositional variation in the Talkeetna gabbronorites, we performed a principal component analysis on the major element oxides (in weight percent) from 92 individual gabbronorite samples. The first principal component of the gabbronorite suite was found to be: 0.84 SiO_2 − 0.08 Al_2O_3 − 0.39 MgO − 0.18 FeO* − 0.30 CaO + 0.11 Na_2O, which describes 54% of the total variance in the system. This vector basically corresponds to variations in plagioclase proportion and composition, with abundant, albitic plagioclase at the high SiO_2 end, and less abundant, anorthitic plagioclase on the low SiO_2 end. This is similar to the fractionation vector for the gabbronorites investigated by *Greene et al.* [2006].

[30] To investigate the sensitivity of crustal density to compositional variations along this trend, we calculated the garnet mode and bulk density for a suite of synthetic gabbronorite compositions constructed by adding or subtracting linear combinations of the first principal component to the average Talkeetna gabbronorite composition. Figure 7 shows that for 800°C and 1 GPa the average Talkeetna gabbronorite lies at the neutrally buoyant point along a nearly linear trend relating increasing SiO_2 content to decreasing density. This implies that the average gabbronorite remaining in the Talkeetna section is neutrally buoyant, and that evolved gabbronorites with albite-rich plagioclase are positively buoyant. In contrast, more primitive gabbronorites with high anorthite plagioclase and a larger proportion of pyroxene were negatively buoyant with respect to residual peridotite. Thus the missing primitive gabbronorites were negatively buoyant with respect to the underlying mantle in the Talkeetna section.

[31] We also examined the sensitivity of the garnet mode and density to variations in the Mg # of the average Talkeetna gabbronorite, with no changes in the other major element oxides. A set of calculations were performed in

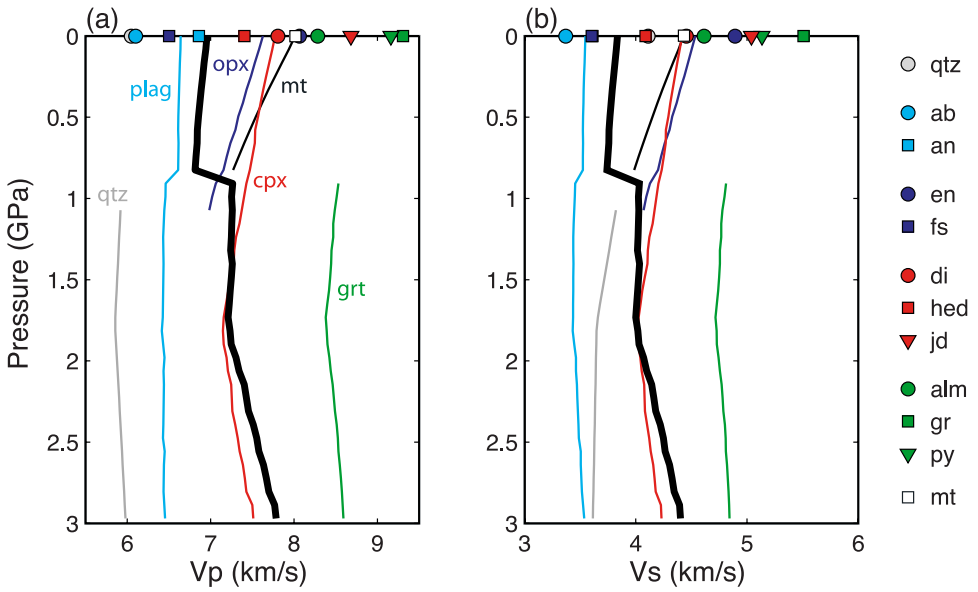

Figure 8. Calculated (a) P wave and (b) S wave velocities for crystallizing mineral phases (thin colored lines) and bulk composition (thick black line) for the average Talkeetna gabbronorite along an 800°C geotherm. Colored symbols illustrate velocity of individual mineral end-members at 15°C and 1 bar. Note that the bulk velocity is sensitive to both the minerals phases that are present as well as the mineral compositions.

which the relative MgO and FeO* content of the gabbronorite composition was varied to produce a series of synthetic compositions with Mg #s ranging from 50–100 (Figures 7b and 7d). At 800°C and 1 GPa, the garnet mode remains relatively constant at ~40 vol % for Mg # between 50 and 90, with garnet replaced by spinel only for Mg # > 90. Similarly the gabbronorite density is relatively insensitive to variations in Mg # between 50 and 90. This implies that while variations in bulk composition along the principal eigenvector strongly influence density, changes in Mg # alone have little influence on lower crustal stability.

5. Seismic Structure of the Lower Talkeetna Crust

[32] One difficulty in inferring ongoing geologic processes from accreted terranes such as the Talkeetna section is assessing to what extent these terranes are representative of modern volcanic arcs. Also, exposures of ancient crustal sections are the time-integrated end-products of many diachronous processes. Seismic data provide one of the primary clues to the composition of in situ lower crust at active arcs at one specific time. Thus, to compare the lower Talkeetna crust with modern volcanic arcs, we used the equilibrium mineral assemblages to estimate the seismic structure of the Talkeetna lower crust. Figure 8 illustrates the calculated P wave velocity (Vp) and S wave velocity (Vs) for the crystallizing mineral phases as well as the bulk velocity for the average Talkeetna gabbronorite composition along an 800°C geotherm. Bulk velocity is calculated as the average of the upper and lower Hashin-Shtrikman bounds, which are typically tighter than 0.05–0.1 km/s for lower crustal compositions [*Behn and Kelemen*, 2003; *Korenaga et al.*, 2002]. To assess the sensitivity of the predicted velocities to temperature, we calculated Vp, Vs, and Vp/Vs ratio versus depth along 800°C and 1000°C geotherms for the average gabbronorite and pyroxenite compositions (Figure 9). At 1 GPa the average Talkeetna gabbronorite has Vp = 6.7–7.3 km/s and Vs = 3.6–4.0 km/s, while the Tonsina pyroxenite composition has Vp = 7.3–7.6 km/s and Vs = 4.2–4.4 km/s. These calculated velocities agree well with laboratory measurements of Vp performed at 1 GPa for gabbroic and ultramafic compositions after correcting for the effects of temperature using typical temperature derivatives for mafic rocks [*Christensen and Mooney*, 1995]. It is interesting that while the gabbronorite and pyroxenite compositions have similar Vp under lower crustal conditions, they are characterized by very different Vs and Vp/Vs structures (Figure 9). This provides a potentially powerful criterion for distinguishing between gabbronorite and pyroxenite compositions in seismic experiments in which high-quality Vp and Vs data are available.

5.1. Relationship between Density and Seismic Velocity

[33] To constrain the relationship between density and seismic velocity for over a range of lower crustal compositions, we calculated density, Vp, and Vs under anhydrous conditions for a suite of arc plutonic rock samples from the Talkeetna section, Mount Stuart batholith [*Erikson*, 1977; *Kelemen and Ghiorso*, 1986], Kohistan [*Kelemen et al.*, 2003a, and references cited therein], Ladakh [*Honegger et al.*, 1982; *Lee et al.*, 2006], and the Aleutians [*Kelemen et al.*, 2003c, and references cited therein]. Figures 10a, 10b, 11a,and 11b illustrate the relationship between density, Vp, and Vp/Vs for arc lower crust (800°C, 1 GPa) and arc middle crust (475°C, 0.5 GPa), respectively. As was shown by *Birch* [1960, 1961], density and Vp are nearly linearly related at both midcrustal and lower crustal conditions. In contrast, Vp/Vs is a complex function of density with the largest Vp/Vs ratios found at densities between 2800–3000 kg/m^3 (Figures 10b and 11b). These density-velocity systematics illustrate the utility of combining Vp and Vs

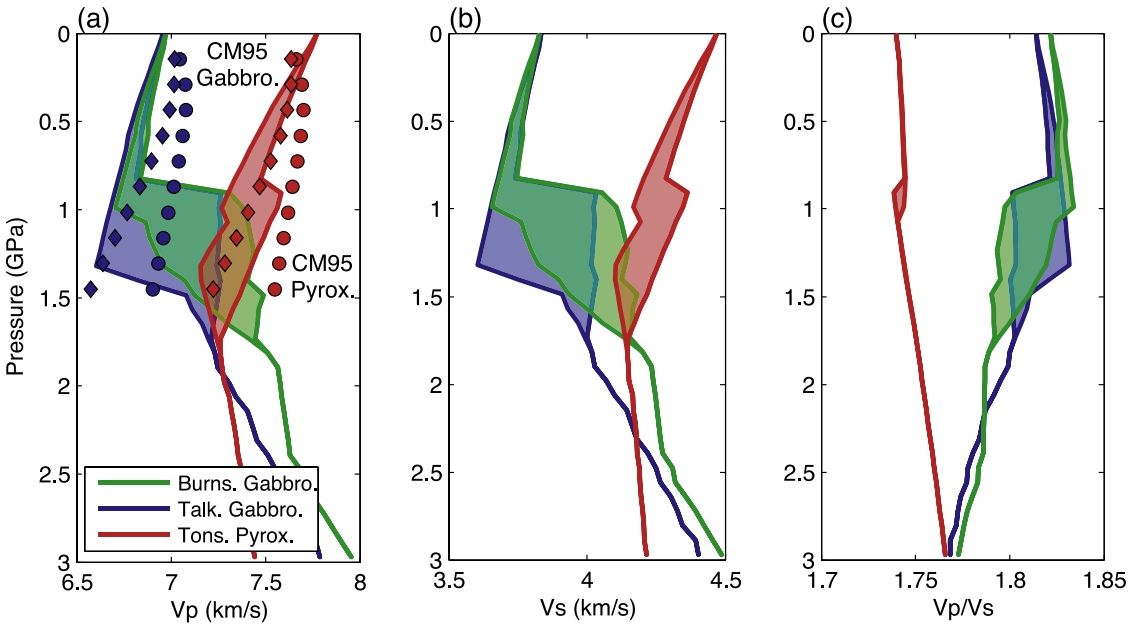

Figure 9. (a) Vp, (b) Vs, and (c) Vp/Vs calculated as a function of pressure for the *Burns* [1983] Tonsina gabbronorite (green), Talkeetna gabbronorite (blue), and Tonsina pyroxenite (red) compositions. Colored regions indicate the range of seismic velocities defined by the 800°C and 1000°C geotherms, with slower velocities corresponding to higher temperatures. Symbols in (a) show laboratory-determined Vp for gabbronorite (blue) and pyroxenite (red) compositions along a ~900°C (circles) and 550°C (diamonds) geotherms [*Christensen and Mooney*, 1995]. Note the large difference in Vp/Vs ratio at 1 GPa between the pyroxenite and gabbronorite compositions.

data to distinguish between gabbronorite (Vp = 7.0–7.7 km/s, Vp/Vs = 1.78–1.82) and pyroxenite (Vp = 7.3–7.7 km/s, Vp/Vs = 1.70–1.75) compositions in the lower crust. Similarly, *Niu et al.* [2004] and *Wagner et al.* [2005, 2006] have shown that Vp/Vs can be used to resolve compositional differences in the upper mantle. Thus it is critical that future seismic studies at arcs focus on resolving both Vp and Vs in order to more accurately characterize the composition of the crust and upper mantle.

[34] To compare the density-Vp relationship for lower crustal rocks to that of the underlying mantle, we calculated density and Vp for the average Talkeetna harzburgite composition (Table 1) [*Kelemen et al.*, 2003a]. At 800°C and 1 GPa the Talkeetna harzburgite was found to have a density of 3250 kg/m^3 and P wave velocity of 7.8 km/s. These values are consistent with laboratory measurements on dunite and harzburgite at 1 GPa after correcting for temperature [*Christensen and Mooney*, 1995], as well as with uppermost mantle P wave velocities beneath arcs [e.g., *Shillington et al.*, 2004, and references cited therein].

[35] Comparing the harzburgite properties to the density-Vp relationship for lower crustal rocks, we find that in order for the lower crustal density to exceed the harzburgite density, crustal P wave velocities must be greater than ~7.4 km/s (Figure 10a). This relationship holds for gabbroic rocks and pyroxenites. In section 6.2 we discuss the implications of this relationship for the stability of arc lower crust based on seismic data from modern arcs.

5.2. Seismic Velocity Structure and Lower Crustal Composition

[36] Seismic data are often used to infer the composition of arc lower crust. In particular, "high" (6.9–7.3 km/s, see Table 3) P wave velocities observed in the lower crust are typically attributed to mafic compositions [e.g.,

Figure 10. Comparison of (a) calculated Vp and density and (b) calculated Vp/Vs and density for a range of arc compositions at lower crustal conditions (800°C and 1 GPa). (c–f) Calculated Vp versus SiO_2, Al_2O_3, Mg #, and Na_2O, respectively. Grey band indicates lower crustal P wave velocities (7.3–7.7 km/s) for the central Aleutian island arc from *Shillington et al.* [2004]. Symbols represent compositions appropriate for arc crust including Talkeetna gabbronorites (blue circles) [*Burns*, 1985; *DeBari and Coleman*, 1989; *Greene et al.*, 2006; *Kelemen et al.*, 2003a], Klanelneechina diorites (pink circles) [*Kelemen et al.*, 2003a], Mount Stuart plutonic rocks (light blue squares) [*Erikson*, 1977; *Kelemen and Ghiorso*, 1986], Talkeetna quartz diorites (green circles) [*Kelemen et al.*, 2003a], Tonsina pyroxenites (red circles) [*Kelemen et al.*, 2003a], Aleutian plutonic rocks (yellow triangles) [*Kelemen et al.*, 2003c, and references cited therein], Kohistan quartz diorites (grey squares) [*Kelemen et al.*, 2003a, and references cited therein], Ladakh quartz diorites (white circles) [*Honegger et al.*, 1982], Sierra Nevada pyroxenite samples (pink triangles) [*Lee et al.*, 2006], average Talkeetna harzburgite (black star) [*Kelemen et al.*, 2003a], and estimates for the average middle and lower continental crust (white stars) [*Dupuy et al.*, 1979; *Rudnick and Fountain*, 1995; *Rudnick and Presper*, 1990; *Shaw et al.*, 1986; *Taylor and McLennan*, 1985; *Weaver and Tarney*, 1984; *Wedepohl*, 1994].

Fliedner and Klemperer, 1999, 2000; *Holbrook et al.*, 1999; *Shillington et al.*, 2004].

[37] To quantify the relationship between seismic velocity and lower crustal composition, we used the suite of arc crust samples described above and compared the calculated Vp to major element chemistry at lower and midcrustal conditions (see Figures 10c–10f and 11c–11f, respectively). Note that this comparison differs from similar comparisons by *Behn and Kelemen* [2003] because here we restrict our calculations to a limited suite of plutonic rocks from ancient and modern arcs, whereas in the previous paper we considered the compositional space defined by all igneous rocks. Here, we find that Vp and SiO_2 are relatively well correlated in the midcrust and at lower crustal conditions with $SiO_2 > 55$ wt %. However, the range of SiO_2 contents corresponding to a specific value of Vp is greater than or equal to ±5 wt %, implying that observations of P wave velocity provide a relatively weak constraint on SiO_2 content. Furthermore for $SiO_2 < 55$ wt % and P,T conditions appropriate for

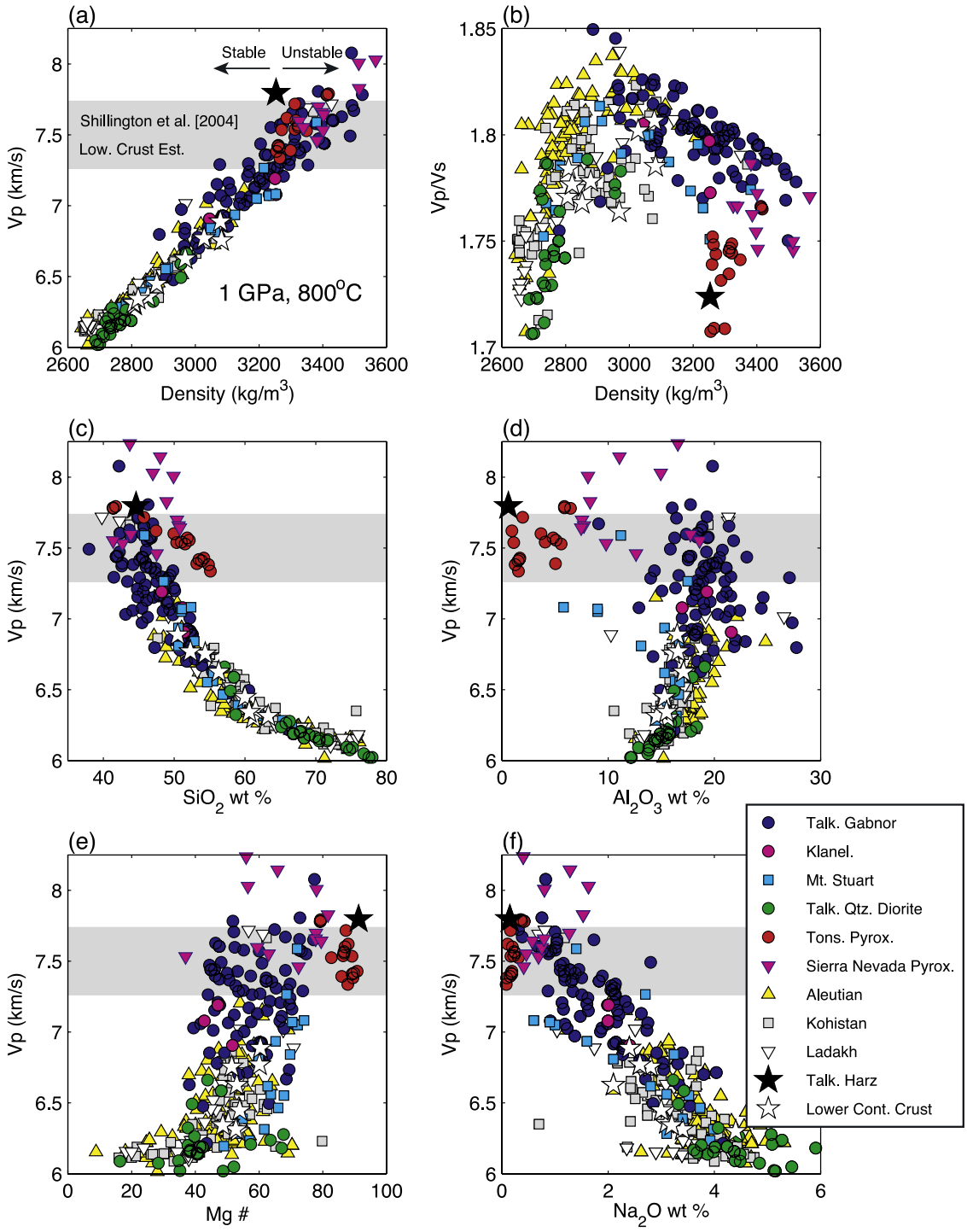

Figure 10

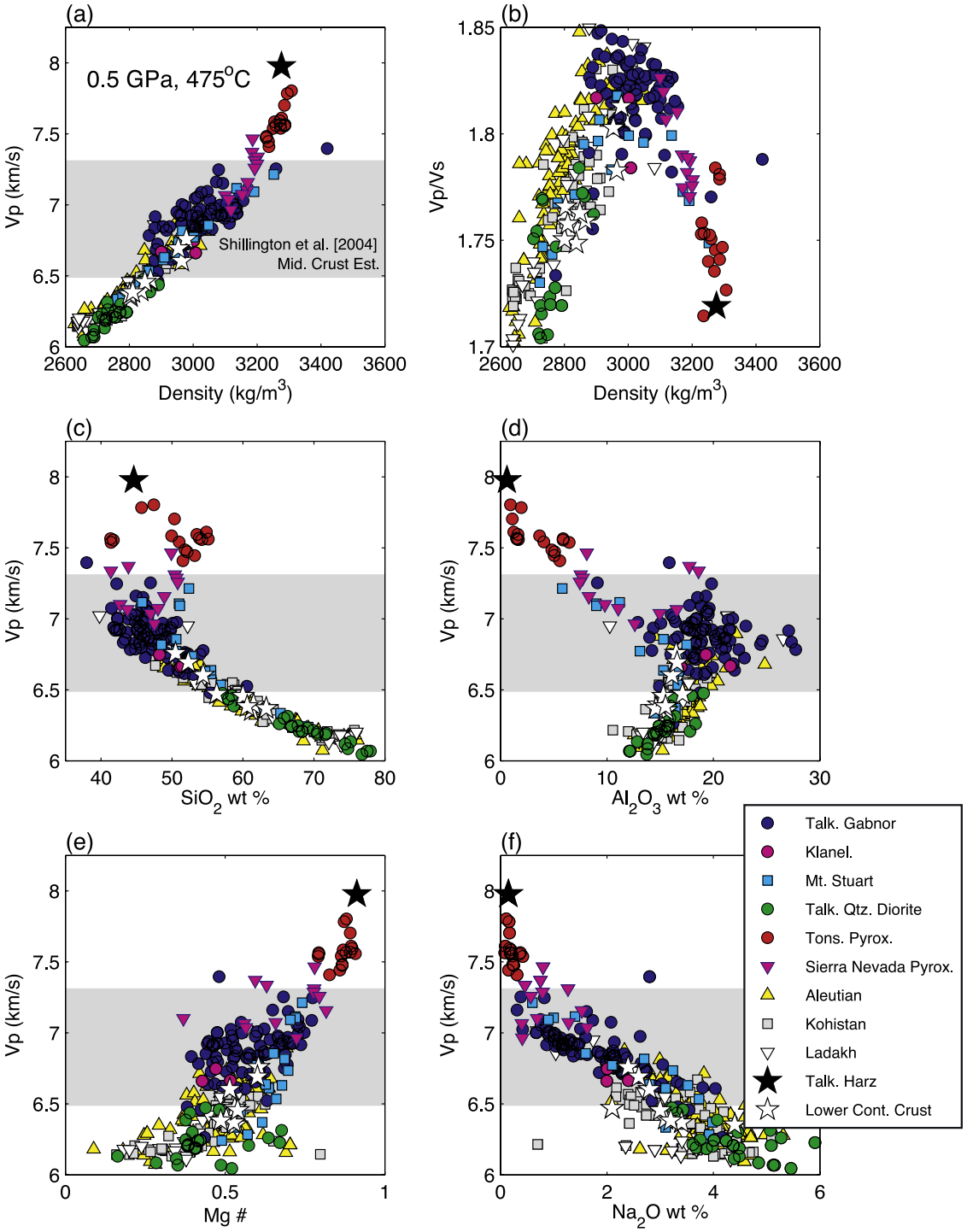

Figure 11. Comparison of (a) calculated Vp and density and (b) calculated Vp/Vs and density for a range of arc compositions at midcrustal conditions (475°C and 0.5 GPa). (c–f) Calculated Vp versus SiO_2, Al_2O_3, Mg #, and Na_2O, respectively. Grey band indicates midcrustal P wave velocities (6.5–7.3 km/s) for the central Aleutians island arc from *Shillington et al.* [2004]. See Figure 10 for full description of symbols and calculations.

the arc lower crust, Vp is a very weak function of SiO_2 content, so that velocities of 6.8–7.7 are consistent with SiO_2 contents of 45–50 wt % (Figure 10c). This implies that for the range of P wave velocities typically observed in arc lower crust (6.9–7.3 km/s), the variations in velocity may be largely independent of SiO_2 content. Although here we calculate Vp for plutonic rock samples specifically from arcs, our results are consistent with previous calculations by *Behn and Kelemen* [2003], who found that Vp is a poor indicator of major element chemistry in lower crustal rocks.

Table 3. Seismic Vp in Arc Middle and Lower Crust

	Middle Crust Vp, km/s	Lower Crust Vp, km/s
Izu-Bonin[a]	6.0–6.3	7.1–7.3
Central Aleutians, line A1[b]	6.5–6.8	6.9–7.3
Central Aleutians, line A3[c]	6.2–6.8	6.8–6.9
Central Aleutians (arc parallel), line A2[d]	6.8–7.3	7.3–7.7
Central Aleutians (arc parallel), line A2[e]	6.4–6.8	6.6–7.3

[a]*Suyehiro et al.* [1996].
[b]*Holbrook et al.* [1999].
[c]*Lizarralde et al* [2002].
[d]*Shillington et al.* [2004].
[e]*Fliedner and Klemperer* [1999, 2000].

5.3. Influence of Melt on Lower Crustal Density and Seismic Structure

[38] The calculations described above assume subsolidus mineral assemblages for the lower crust. However, the high equilibration temperatures and finite water contents characteristic of Talkeetna gabbronorite samples may indicate that there is partial melt present in arc lower crust near the Moho. To estimate the proportion of melt that might be present, we used the melting model of *Holland and Powell* [2001] and calculated melt fraction as a function of temperature and water content at 1 GPa for the average gabbronorite and pyroxenite compositions (Figure 12). The *Holland and Powell* [2001] model was used instead of pMELTS [*Ghiorso et al.*, 2002] because it more closely reproduces the observed melt fractions and solid mineral assemblages found in laboratory melting experiments on hydrous gabbronorite [e.g., *Müntener et al.*, 2001]. These calculations show that the average Talkeetna gabbronorite crosses the dry solidus at ~980°C and can produce up to 7–8% melt at 1000°C and 0.5 wt % H_2O. On the other hand, the average pyroxenite is not predicted to melt under any conditions for temperatures <1025°C and water contents ≤0.5 wt %.

[39] While small degrees of melting typically have little influence on the solid phase assemblage [*Müntener et al.*, 2001], the presence of melt can strongly influence bulk seismic velocity [e.g., *Mainprice*, 1997; *O'Connell and Budiansky*, 1977; *Schmeling*, 1985]. To assess the influence of melting on density-velocity systematics in arc lower, we compared calculations assuming subsolidus mineral assemblages to calculations incorporating the melting model of *Holland and Powell* [2001] for the suite of gabbronorite and pyroxenite samples shown in Figures 10 and 11. To maximize the potential influence of melting, all calculations were performed under hydrous conditions with 0.5 wt % H_2O.

[40] Figure 13 illustrates the effect of melting on bulk density and Vp at 1 GPa for Moho temperatures of 800°C and 1000°C. In general, the presence of melt has a small influence on bulk density for these lower crustal compositions. The only exception is along the 1000°C geotherm where several samples display a ~100 kg/m^3 increase in density for calculations that include melting. This increase is associated with dehydration during melting, which results in breakdown of hornblende and crystallization of garnet in the residual anhydrous mineral assemblages. The presence of melt has a larger influence on bulk P wave velocity, with slower velocities predicted for calculations with melt present. This, effect is most pronounced for Vp < 6.8 km/s, where melt fractions are typically predicted to be >10%. However, as noted above lower crustal velocities in arcs are generally found to be 6.9–7.3 km/s. Thus it is unlikely that the presence of partial melt significantly alters the density-velocity systematics for compositions in this velocity range.

6. Discussion

6.1. The fO_2-"Barometry"

[41] We have shown that the quartz-, olivine-, garnet-free mineral assemblages characteristic of gabbronorites from the Talkeetna section as well as those from the similar Kohistan section in Pakistan [*Kelemen et al.*, 2003a] define a narrow range of fO_2 conditions centered on NNO+2 (±1 log unit). These calculations are in agreement with earlier results by *Frost and Lindsley* [1992], who used equilibria between Fe-Ti oxides, pyroxenes, olivine, and quartz to predict the P, T, and fO_2 activity in mafic, arc-related gabbros from Bear Mountain. Specifically, *Frost and Lindsley* [1992] found that for QFM+3 (≈NNO+1) olivine-free/quartz-free mineral assemblages were predicted for $X_{Fe}^{Opx} \approx 0.25$. These values are similar to the FeO in orthopyroxene observed in the Talkeetna gabbronorites [*Greene et al.*, 2006], and thus are consistent with the oxidizing conditions in the lower Talkeetna crust in the range of NNO+1 to NNO+3.

[42] It has long been recognized that arc lavas are oxidized relative to mid-ocean ridge basalts, with MORBs lying near FMQ and arc basalts ranging from NNO to NNO+2 [*Carmichael*, 1991]. In general, more oxidized arc lavas tend to be associated with more hydrous conditions

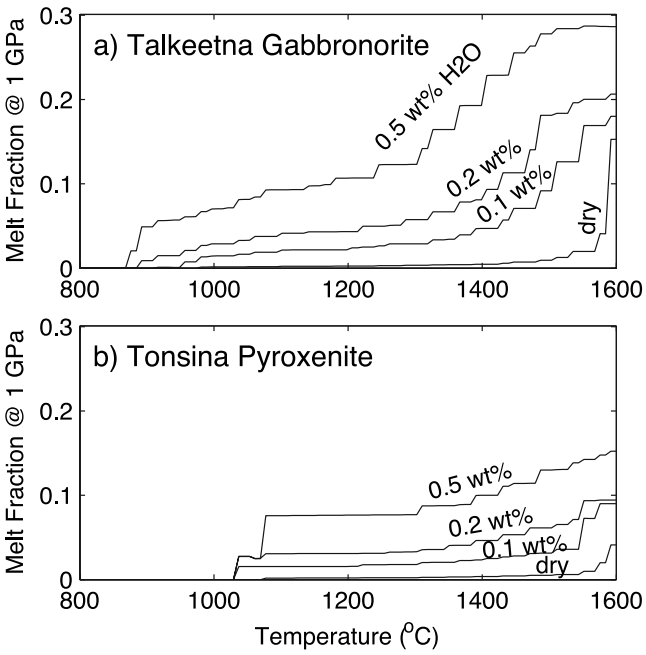

Figure 12. Melt fraction as a function of temperature at 1 GPa for the (a) average Talkeetna gabbronorite and (b) average Tonsina pyroxenite. Melting is calculated using the melt model of *Holland and Powell* [2001]. Under hydrous conditions the gabbronorite is predicted to melt 5–7% at temperatures of 900–1000°C. However, no melt is predicted for the pyroxenite at temperatures <1000°C.

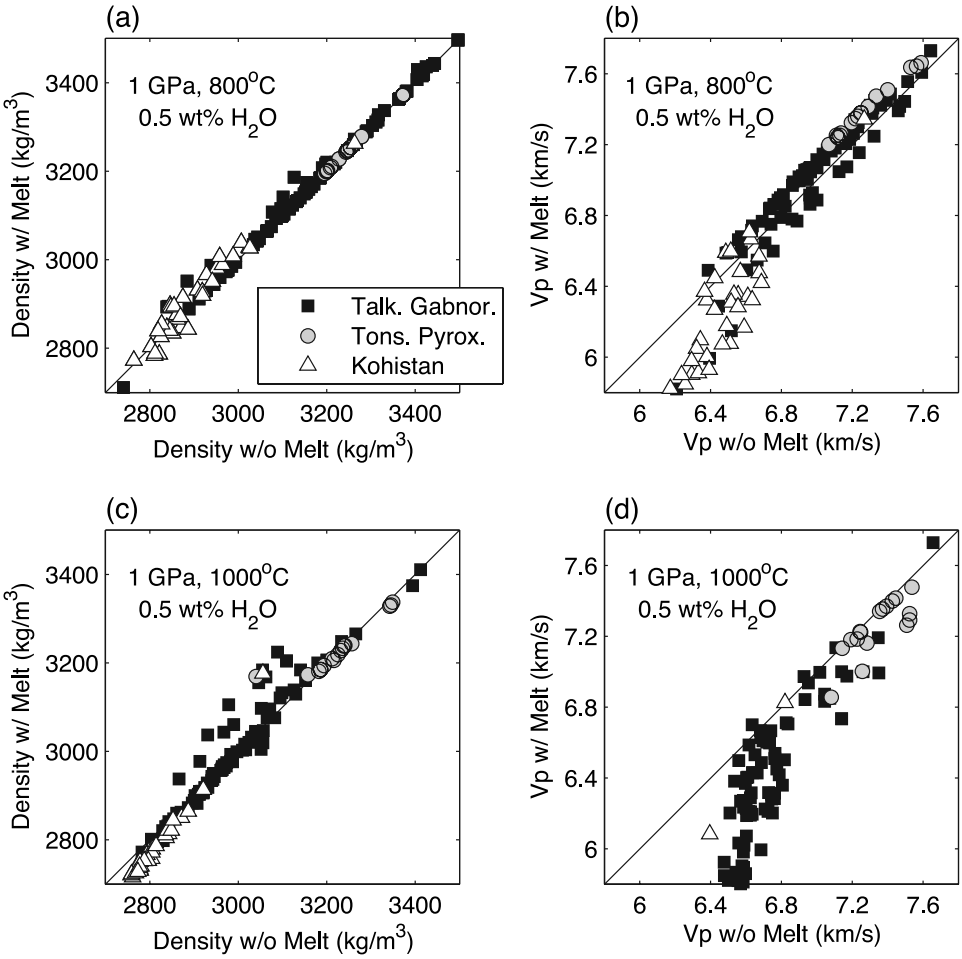

Figure 13. Effect of melting on density and Vp for a range of gabbronorite and pyroxenite compositions from the Talkeetna and Kohistan arc sections. Calculations are performed at (a,b) 800°C and (c,d) 1000°C and 1 GPa and assume 0.5 wt % H_2O. Effect of melt on Vp is calculated after *Mainprice* [1997], assuming spherical melt inclusions and a melt bulk modulus of 15 GPa. For seismic velocities typical of arc lower crust (6.9–7.3 km/s) melting has a small influence on both density and Vp.

and this correlation has been attributed to the reaction: $2FeO + H_2O \leftrightarrow Fe_2O_3 + H_2$ [e.g., *Arculus*, 1994; *Wood et al.*, 1990]. Our results build on these earlier observations by providing a useful fO_2 barometer than can be applied based solely on the observed mineral assemblages in arc gabbronorites. Figure 3 shows that the upper and lower bounds on fO_2 are defined by the stability fields of quartz and olivine, respectively, and are relatively insensitive to variations in temperature and pressure. Thus the presence or absence of each of these minerals provides a first-order proxy for the fO_2 conditions during igneous crystallization.

6.2. Foundering of the Talkeetna Lower Crust

[43] The calculations described above provide a basis for interpreting the stability of the lower crust in the Talkeetna section. For a typical arc-like geotherm the average Talkeetna gabbronorite is neutrally or slightly positively buoyant relative to the underlying mantle for pressures above 1.5 GPa (Figure 4). However, the gabbronorite density is controlled by the stability of garnet and is highly sensitive to variations in temperature, major element chemistry, and H_2O content. Gabbronorites that are more primitive than the average Talkeetna composition crystallize a larger garnet mode resulting in a negatively buoyant ($\rho_{crust} - \rho_{mantle} \geq 100$ kg/m^3) mineral assemblage relative to the underlying mantle (see Figures 4 and 7). In contrast to the gabbronorite, the average pyroxenite density is relatively insensitive to variations in temperature, composition, and H_2O content and is found to be slightly negatively buoyant ($\rho_{crust} - \rho_{mantle} \approx 70$ kg/m^3) for pressures greater than 0.8 GPa on likely arc geotherms (Figures 4 and 5).

[44] Given the expected low viscosity of lower crustal mineral and upper mantle assemblages at temperatures of 800°C–1000°C, *Jull and Kelemen* [2001] calculated convective instability times of 10^4–10^6 years for density contrasts in the range of 50–200 kg/m^3. In this parameter range, the predicted instability times are nearly independent of the magnitude of the density contrast between the crust and mantle [*Jull and Kelemen*, 2001], implying that even in situations where the density contrast between the lower crust and upper mantle is relatively small, crustal foundering can occur on timescales $\leq 10^6$ years.

[45] The calculated lower crustal densities combined with field observations provide two potential scenarios for the evolution of Talkeetna lower crust. In the first model,

gabbronorites with Mg # < 75, plus relatively high Na_2O and SiO_2, form lower crustal mineral assemblages that are neutrally or positively buoyant relative to the underlying mantle, consistent with the composition of the majority of gabbronorites preserved in the Talkeetna section. More primitive gabbronorites and pyroxenites with Mg # > 80, accompanied by lower Na_2O and SiO_2, likely formed lower crustal mineral assemblages that were denser than the underlying, residual mantle peridotite. Such primitive gabbronorite and pyroxenite compositions are only observed in isolated locations of the Talkeetna section and are compositionally equivalent to the rocks predicted to be missing from the lower crust based on fractional crystallization modeling of the Talkeetna lavas [*Greene et al.*, 2006; *Kelemen et al.*, 2003a]. Intriguingly, no primitive gabbronorites with Mg # > 80 are observed in the Kohistan arc section, providing further evidence that these compositions are convectively unstable because they are dense relative to the underlying mantle.

[46] An alternative explanation for the missing primitive gabbronorites and pyroxenites in the Talkeetna lower crust is that these high Mg # rocks crystallize beneath the Moho, perhaps in melt lenses surrounded by residual mantle peridotite. In this scenario, the uppermost mantle would consist of harzburgite intermixed with pyroxenite and limited amounts of gabbronorite. The limited mantle exposure in the Talkeetna section is not sufficient to test this hypothesis. Furthermore, if the pyroxenite layers were relatively thin, they would be extremely difficult to detect in seismic refraction experiments at modern arcs.

6.3. Comparison to Seismic Structure at Modern Arcs

[47] Interpretation of seismic sections for active arcs is aided by geological data from ancient, exposed crustal sections of the accreted Jurassic Talkeetna arc in south central Alaska [e.g., *Plafker et al.*, 1989] and Cretaceous Kohistan arc in northern Pakistan [e.g., *Tahirkheli*, 1979]. The potential seismic sections in Figure 14 are based on our recent Talkeetna Arc Continental Dynamics project. Specifically, *Kelemen et al.* [2006] used the thermobarometric data of *Hacker et al.* [2006] together with geochemical averages [*Kelemen et al.*, 2003a] to construct several possible, end-member crustal sections through the Talkeetna arc.

[48] The Talkeetna section preserves residual mantle peridotites at the base (south) through a northward dipping sequence of lower crustal gabbroic rocks to an extensive section of arc volcanics at the top (north). The volcanics are primarily intruded by felsic plutonic rocks. However, the section has been tectonically thinned, mainly along what are now steeply dipping, right lateral strike-slip faults. Thus we must rely on thermobaromatric data to constrain the proportions of different rock types in the section prior to thinning.

[49] A key variable in determining the bulk composition of the Talkeetna arc crust is the proportion of felsic versus mafic plutonic rocks. The new thermobarometric data of *Hacker et al.* [2006] indicate that there is a substantial gap in outcrop between tonalities and quartz diorites emplaced at 5 to 9 km and gabbronorites crystallized at 17 to 24 km. Thus there is a missing, 8 to 19 km thick, midcrustal section, which could be composed of gabbronorite, felsic plutonic rocks, or a mixture of the two. Additional uncertainties are that the felsic plutonic rocks and lower crustal composition are different in different places. Tonalites and quartz diorites in the Klanelneechina klippe, some of which include garnet and record pressures of about 0.7 GPa, are very different in composition from gabbronorites recording similar pressures elsewhere in the Talkeetna section.

[50] Sections A through D in Figure 14 represent a few possible end-member crustal sections, from most felsic to most mafic, constructed using the constraints outlined above. We note that our calculations ignore the potential effects of porosity at shallow crustal levels, which will significantly reduce Vp at pressures less than 0.4 GPa. Superimposed on the calculated seismic sections are velocity profiles A1 [*Holbrook et al.*, 1999] and A3 [*Lizarralde et al.*, 2002] from refraction data in the Aleutian arc. Models C and D most closely resemble the structure of the Aleutian velocity structure with Vp > 6.8 km/s at pressures above 0.4 GPa.

6.4. Lower Crustal Stability in Modern Arcs

[51] As discussed in section 5.1, for arc lower crust to be unstable relative to the underlying mantle, lower crustal P wave velocities must exceed ~7.4 km/s (Figure 10a). Using this criterion, we compiled seismic refraction data from modern arcs (Table 3) and found that typical lower crustal velocities range from 6.9 to 7.3 km/s. Thus we conclude that in situ lower crust beneath most modern arcs is convectively stable and that either unstable material founders rapidly on geologic timescales or high Vp plutonic rocks crystallize beneath the base of the crust or high Vp rocks do not form at all.

[52] This observation is particularly relevant for studies that interpret the formation of the continental crust via the accretion of arc terranes. Specifically, studies that interpret the average composition of arc crust from seismic data typically infer a more mafic composition for the arc relative to average continental crust [e.g., *Holbrook et al.*, 1999; *Shillington et al.*, 2004]. This discrepancy requires that a large proportion of arc lower crust with Vp = 6.9–7.3 km/s, and corresponding SiO_2 contents less than 55 wt %, be removed. However, the results of this study indicate that foundering of material with Vp < 7.4 km/s is unlikely.

[53] Implicit in the apparent discrepancy between arc composition and average continental crust is the assumption that major element chemistry can be accurately inferred from seismic data. Yet the results of this study as well as those of *Behn and Kelemen* [2003] clearly demonstrate that seismic P wave velocity is a weak constraint on crustal composition. For example, Figure 10c shows that SiO_2 contents ranging from 43 to 55 wt % are consistent with lower crustal velocities of 6.9–7.3 km/s. Furthermore, *Behn and Kelemen* [2003] showed that by formally inverting Vp for composition along a warm continental geotherm, a velocity of 7.1 ± 0.2 km/s resulted in a range in SiO_2 content of 43–63 wt %. Thus, on the basis of P wave velocities alone one cannot conclude that average composition of arc crust is significantly different than that of continental crust.

[54] One region where seismic velocities do imply unstable material is in the central Aleutians, where *Shillington et al.* [2004] find a ~100 km along-strike section of the arc lower crust with Vp = 7.3–7.7 km/s. It should be noted that *Fliedner and Klemperer* [1999, 2000], analyzed refraction

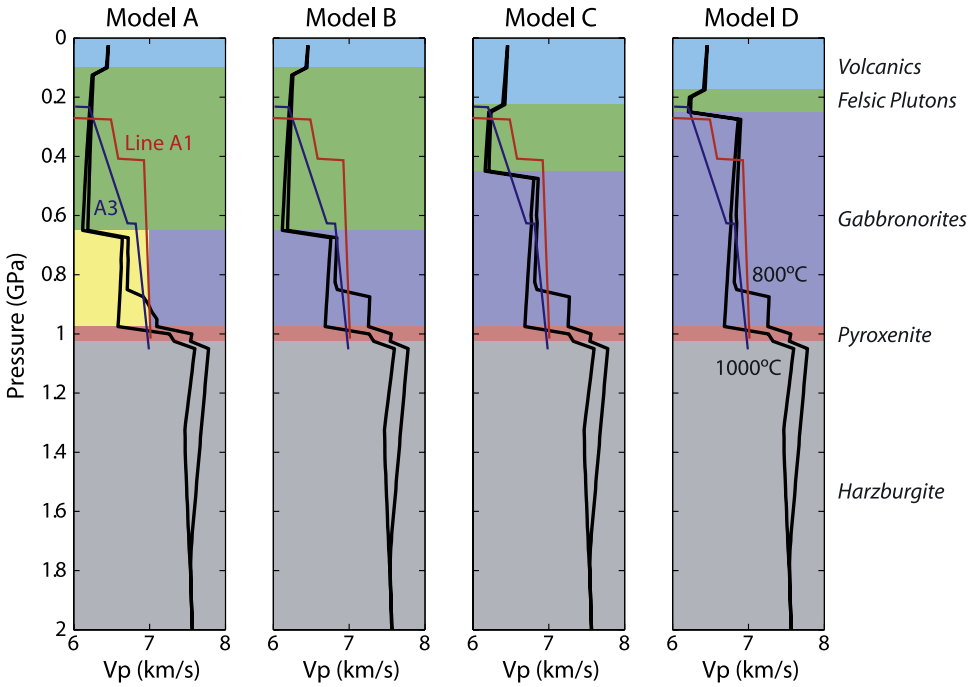

Figure 14. Calculated seismic sections for 4 end-member crustal models for the Talkeetna arc section from *Kelemen et al.* [2006] (see text for discussion). Velocities are calculated along an 800°C and 1000°C geotherm, using the average composition of the Talkeetna volcanics (light blue), felsic plutons (green), gabbronorites (blue), tonalities and quartz diorties from the Klanelneechena klippe (yellow), pyroxenites (red), and harzburgite (grey) [*Kelemen et al.*, 2003a]. In model A, the composition of the lower crust is calculated as the average composition of the Talkeetna gabbronorite and Klanelneechena tonalities and quartz diorites. Seismic velocity profiles from refraction lines A1 [*Holbrook et al.*, 1999] and A3 [*Lizarralde et al.*, 2002] in the Aleutians are shown by the red and blue curves, respectively.

data along the same line as *Shillington et al.* [2004], and found lower crustal velocities of only 6.8–7.3 km/s in the same region, though they reported sub-Moho velocities in the 7.5 to 7.8 km/s range. The differences between these two models are probably related to trade-offs between crustal velocity and crustal thickness, as well as difficulties in interpreting incoming phases along an arc-parallel line with a complex three-dimensional (3-D) geometry, and/or to the method used to identify the Moho. However, if velocities approaching 7.7 km/s are indeed representative of the lower crust in this region, they probably correspond to ultramafic cumulates or garnet granulites [*Behn and Kelemen*, 2003; *Christensen and Mooney*, 1995; *Fliedner and Klemperer*, 1999] similar to the most primitive gabbronorites and pyroxenites observed in the Talkeetna section (Figure 10). This portion of the Aleutian arc would therefore represent a region where rocks denser than underlying mantle peridotite have recently crystallized in the lower crust, but have not yet foundered.

7. Conclusions

[55] Field observations from the Talkeetna arc section in south central Alaska [*Kelemen et al.*, 2003a], combined with modeling of fractionation of primitive arc magmas [*Greene et al.*, 2006], indicate that large amounts of primitive gabbronorite and pyroxenite are missing from the lower crust. One longstanding model for the removal of this material is foundering of dense cumulates from the base of the crust [e.g., *Arndt and Goldstein*, 1989; *DeBari and Sleep*, 1991; *Ducea and Saleeby*, 1996, 1998; *Herzberg et al.*, 1983; *Kay and Kay*, 1988, 1985; *Kelemen et al.*, 2003a; *Lee et al.*, 2000; *Saleeby et al.*, 2003; *Turcotte*, 1989]. To evaluate the stability of the lower Talkeetna crust, we performed calculations of phase equilibria for a range of gabbroic and ultramafic compositions at P, T, oxygen fugacity (fO_2), and H_2O contents appropriate for arc lower crust. In particular, the quartz-olivine-garnet-free mineral assemblage observed in the Talkeetna gabbronorites (and in the similar Kohistan section in Pakistan) was found to define a narrow range of fO_2 centered on NNO+2 (±1 log unit).

[56] Densities determined from the equilibrium mineral assemblages indicate that the gabbronorites which compose the majority of the Talkeetna lower crust are neutrally or slightly positively buoyant relative to the underlying mantle harzburgite, while the thin layer (~500 m thick) of pyroxenites at the base of the crust are slightly negatively buoyant. Furthermore, we estimate that the missing gabbroic and ultramafic rocks from the Talkeetna section were denser than the underlying mantle. On the basis of these calculations we conclude that the Talkeetna lower crust is likely in an equilibrium configuration in which the lower crust is convectively stable relative to the underlying mantle and the denser, more primitive cumulates have either been removed via foundering or crystallized beneath the base of the crust.

[57] Generalizing our results to active arcs, we used the calculated phase equilibria to assess the relationship be-

tween seismic structure, lower crustal composition, and the stability of arc lower crust. As shown by *Behn and Kelemen* [2003], P wave velocity is a poor indicator of lower crustal composition, and compositions ranging from basaltic to dacitic are allowed for lower crustal velocities of 6.9–7.3 km/s. On the other hand, future seismic studies that integrate high quality Vp and Vs data have the potential to place much tighter constrains on crustal composition and distinguish between gabbroic and ultramafic compositions in the lowermost crust. Finally, we show that P wave velocities > 7.4 km/s are indicative of lower crust that is denser than underlying mantle peridotite, and can become convectively unstable. Seismic refraction studies in modern arcs typically find lower crustal Vp < 7.4 km/s, implying that gravitationally unstable material must founder rapidly on geologic timescales, or the missing high Vp plutonic rocks crystallize beneath the Moho, or the primitive, high density cumulates required to balance the Talkeetna arc liquid line of descent are not required and do not form in most other arcs.

[58] **Acknowledgments.** We thank Jamie Connolly for generously allowing us to use his Perple_X code and for assisting us with our multitude of questions. We would like to thank Brad Hacker, Andrew Greene, Susan Debari, Matt Rioux, Dan Lizarralde, Greg Hirth, and Tim Grove for their many helpful comments and discussions at various stages during this project. We are grateful to Brad Hacker and Cin-Ty Lee for their insightful reviews that helped to clarify many portions of this manuscript. This research was funded in part by NSF grants OCE-0426160, EAR-0409092, OCE-0242233, EAR-0125919, and EAR-9910899.

References

Arculus, R. J. (1994), Aspects of magma genesis in arcs, *Lithos*, *33*, 189–208.

Arndt, N. T., and S. L. Goldstein (1989), An open boundary between lower continental crust and mantle: Its role in crust formation and crustal recycling, *Tectonophysics*, *161*, 201–212.

Austrheim, H. (1998), The influence of fluid and deformation of metamorphism of the deep crust and consequences for geodynamics of collision zones, in *When Continents Collide: Geodynamics and Geochemistry of Ultrahigh-Pressure Rocks*, edited by B. Hacker and J. Liou, pp. 297–323, Springer, New York.

Behn, M. D., and P. B. Kelemen (2003), Relationship between seismic P-wave velocity and the composition of anhydrous igneous and metaigneous rocks, *Geochem. Geophys. Geosyst.*, *4*(5), 1041, doi:10.1029/2002GC000393.

Birch, F. (1960), The velocity of compressional waves in rocks to 10 kilobars: 1, *J. Geophys. Res.*, *65*, 1083–1102.

Birch, F. (1961), The velocity of compressional waves in rocks to 10 kilobars: 2, *J. Geophys. Res.*, *66*, 2199–2224.

Burns, L. E. (1983), The Border Ranges ultramafic and mafic complex: Plutonic core of an intraoceanic island arc, Ph.D. thesis, Stanford Univ., Stanford, Calif.

Burns, L. E. (1985), The Border Ranges ultramafic and mafic complex, south-central Alaska: Cumulate fractionates of island-arc volcanics, *Can. J. Earth Sci.*, *22*, 1020–1038.

Carmichael, I. S. E. (1991), The redox states of basic and silicic magmas: A reflection of their source regions?, *Contrib. Mineral. Petrol.*, *106*, 129–141.

Christensen, N. I., and D. M. Fountain (1975), Constitution of the lower continental crust based on experimental studies of seismic velocities in granulite, *Geol. Soc. Am. Bull.*, *86*, 227–236.

Christensen, N. I., and W. D. Mooney (1995), Seismic velocity structure and composition of the continental crust: A global view, *J. Geophys. Res.*, *100*, 9761–9788.

Connolly, J. A. D. (1990), Multivariable phase diagrams: An algorithm based on generalized thermodynamics, *Am. J. Sci.*, *290*, 666–718.

Connolly, J. A. D. (2005), Computation of phase equilibria by linear programming: A tool for geodynamic modeling and its application to subduction zone decarbonation, *Earth Planet. Sci. Lett.*, *236*, 524–541.

DeBari, S. M., and R. G. Coleman (1989), Examination of the deep levels of an island arc: Evidence from Tonsina Ultramafic-Mafic Assemblage, Tonsina, Alaska, *J. Geophys. Res.*, *94*, 4373–4391.

DeBari, S. M., and N. H. Sleep (1991), High-Mg, low-Al bulk composition of the Talkeetna island arc, Alaska: Implications for primary magmas and the nature of arc crust, *Geol. Soc. Am. Bull.*, *103*, 37–47.

Ducea, M., and J. Saleeby (1996), Buoyancy sources for a large, unrooted mountain range, the Sierra Nevada, California: Evidence from xenolith thermobarometry, *J. Geophys. Res.*, *101*, 8229–8244.

Ducea, M., and J. Saleeby (1998), A case for delamination of the deep batholithic crust beneath the Sierra Nevada, California, *Int. Geol. Rev.*, *40*, 78–93.

Dupuy, C., et al. (1979), The lower continental crust of the Massif Central (Bournac, France): With special reference to REE, U and Th composition, evolution, heat-flow production, *Phys. Chem. Earth*, *11*, 401–415.

Erikson, E. H., Jr. (1977), Petrology and petrogenesis of the Mount Stuart Batholith: Plutonic equivalent of the high-alumina basalt association?, *Contrib. Mineral. Petrol.*, *60*, 183–207.

Fliedner, M. M., and S. L. Klemperer (1999), Structure of an island-arc: Wide-angle seismic studies in the eastern Aleutian Islands, Alaska, *J. Geophys. Res.*, *104*, 10,667–10,694.

Fliedner, M. M., and S. L. Klemperer (2000), Crustal structure transition from oceanic arc to continental arc, eastern Aleutian Islands and Alaska Peninsula, *Earth Planet. Sci. Lett.*, *179*, 567–579.

Frost, B. R., and D. H. Lindsley (1992), Equilibria among Fe-Ti oxides, pyroxenes, olivine, and quartz: Part II. Application, *Am. Mineral.*, *77*, 1004–1020.

Ghiorso, M. S., M. M. Hirschmann, P. W. Reiners, and V. C. Kress III (2002), The pMELTS: A revision of MELTS for improved calculation of phase relations and major element partitioning related to partial melting of the mantle to 3 GPa, *Geochem. Geophys. Geosyst.*, *3*(5), 1030, doi:10.1029/2001GC000217.

Greene, A. R., S. M. Debari, P. B. Kelemen, J. Blusztajn, and P. D. Clift (2006), A detailed geochemical study of island arc crust: The Talkeetna Arc section, south-central Alaska, *J. Petrol.*, *47*, 1051–1093.

Grove, T. L., D. C. Gerlach, T. W. Sando, and M. B. Baker (1982), Origin of calc-alkaline series lavas at Medicine Lake Volcano by fractionation, assimilation, and mixing, *Contrib. Mineral. Petrol.*, *80*, 160–182.

Hacker, B., E. Gnos, L. Ratschbacher, M. Grove, M. McWilliams, S. V. Sobolev, J. Wan, and W. Zhenhan (2000), Hot dry deep crustal xenoliths from Tibet, *Science*, *287*, 2463–2466.

Hacker, B. R., G. A. Abers, and S. M. Peacock (2003), Subduction factory: 1. Theoretical mineralogy, densities, seismic wave speeds, and H_2O contents, *J. Geophys. Res.*, *108*(B1), 2029, doi:10.1029/2001JB001127.

Hacker, B. R., et al. (2006), Reconstruction of the Talkeetna intra-oceanic arc of Alaska through thermobarometry, paper presented at Arc Genesis and Crustal Evolution, Geol. Soc. of Am., Valdez, Alaska.

Herzberg, C. T., W. S. Fyfe, and M. J. Carr (1983), Density constraints on the formation of the continental Moho and crust, *Contrib. Mineral. Petrol.*, *84*, 1–5.

Holbrook, W. S., D. Lizarralde, S. McGeary, N. Bangs, and J. Diebold (1999), Structure and composition of the Aleutian island arc and implications for continental crustal growth, *Geology*, *27*, 31–34.

Holland, T., and R. Powell (1996), Thermodynamics of order-disorder in minerals: 2. Symmetric formalism applied to solid solutions, *Am. Mineral.*, *81*, 1425–1437.

Holland, T. J. B., and R. Powell (1998), An internally consistent thermodynamic data set for phases of petrological interest, *J. Metamorph. Geol.*, *16*, 309–343.

Holland, T., and R. Powell (2001), Calculation of phase relations involving haplogranitic melts using an internally consistent thermodynamic dataset, *J. Petrol.*, *42*, 673–683.

Honegger, K., V. Dietrich, W. Frank, A. Gansser, M. Thöni, and V. Trommsdorff (1982), Magmatism and metamorphism in the Ladakh Himalayas (the Indus-Tsangpo suture zone), *Earth Planet. Sci. Lett.*, *60*, 253–292.

Jull, M., and P. B. Kelemen (2001), On the conditions for lower crustal convective instability, *J. Geophys. Res.*, *106*, 6423–6446.

Kay, R. W., and S. M. Kay (1988), Crustal recycling and the Aleutian Arc, *Geochim. Cos. Acta*, *52*, 1351–1359.

Kay, R. W., and S. M. Kay (1991), Creation and destruction of lower continental crust, *Geol. Rundsch.*, *80*, 259–278.

Kay, R. W., and S. M. Kay (1993), Delamination and delamination magmatism, *Tectonophysics*, *219*, 177–189.

Kay, S. M., and R. W. Kay (1985), Role of crystal cumulates and the oceanic crust in the formation of the lower crust of the Aleutian Arc, *Geology*, *13*, 461–464.

Kelemen, P. B. (1995), Genesis of high Mg# andesites and the continental crust, *Contrib. Mineral. Petrol.*, *120*, 1–19.

Kelemen, P. B., and M. S. Ghiorso (1986), Assimilation of peridotite in zoned calc-alkaline plutonic complex; evidence from the Big Jim Complex, Washington Cascades, *Contrib. Mineral. Petrol.*, *94*, 12–28.

Kelemen, P. B., K. Hanghøj, and A. R. Greene (2003a), One view of the geochemistry of subduction-related magmatic arcs, with an emphasis on primitive andesite and lower crust, in *The Crust*, edited by R. L. Rudnick, pp. 593–659, Elsevier, New York.

Kelemen, P. B., J. L. Rilling, E. M. Parmentier, L. Mehl, and B. R. Hacker (2003b), Thermal structure due to solid-state flow in the mantle wedge beneath arcs, in *Inside the Subduction Factory*, *Geophys. Monogr. Ser.*, vol. 138, edited by J. Eiler, pp. 293–311, AGU, Washington, D. C.

Kelemen, P. B., G. M. Yogodzinski, and D. W. Scholl (2003c), Along-strike variation in the Aleutian Island Arc: Genesis of high Mg# andesite and implications for continental crust, in *Inside the Subduction Factory*, *Geophys. Monogr. Ser.*, vol. 138, edited by J. Eiler, pp. 223–276, AGU, Washington, D. C.

Kelemen, P. B., et al. (2006), A new mass balance for the Talkeetna arc crustal composition: Comparison with Izu-Bonin and Aleutian arcs, and constraints on crustal genesis, paper presented at Arc Genesis and Crustal Evolution, Geol. Soc. of Am., Valdez, Alaska.

Kelly, R. K., P. B. Kelemen, and M. Jull (2003), Buoyancy of the continental upper mantle, *Geochem. Geophys. Geosyst.*, *4*(2), 1017, doi:10.1029/2002GC000399.

Korenaga, J., P. B. Kelemen, and W. S. Holbrook (2002), Methods for resolving the origin of large igneous provinces from crustal seismology, *J. Geophys. Res.*, *107*(B9), 2178, doi:10.1029/2001JB001030.

Lee, C., Q. Yin, R. L. Rudnick, J. T. Chesley, and S. B. Jacobsen (2000), Osmium isotopic evidence for Mesozoic removal of lithospheric mantle beneath the Sierra Nevada, California, *Science*, *289*, 1912–1916.

Lee, C.-T., X. Cheng, and U. Horodyskyj (2006), The development and refinement of continental arcs by primary basaltic magmatism, garnet pyroxenite accumulation, basaltic recharge and delamination: Insights from the Sierra Nevada, California, *Contrib. Mineral. Petrol.*, *151*, 222–242.

Lizarralde, D., W. S. Holbrook, S. McGeary, N. L. Bangs, and J. B. Diebold (2002), Crustal construction of a volcanic arc, wide-angle seismic results from the western Alaska Peninsula, *J. Geophys. Res.*, *107*(B8), 2164, doi:10.1029/2001JB000230.

Mainprice, D. (1997), Modelling the anisotropic seismic properties of partially molten rocks found at mid-ocean ridges, *Tectonophysics*, *279*, 161–179.

McBirney, A. R., H. P. Taylor, and R. L. Armstrong (1987), Paricutin re-examined: A classic example of crustal assimilation in calc-alkaline magma, *Contrib. Mineral. Petrol.*, *95*, 4–20.

Miller, D. J., and N. I. Christensen (1994), Seismic signature and geochemistry of an island arc: A multidisciplinary study of the Kohistan accreted terrane, northern Pakistan, *J. Geophys. Res.*, *99*, 11,623–11,642.

Müntener, O., P. B. Kelemen, and T. L. Grove (2001), The role of H_2O and composition on the genesis of igneous pyroxenites: An experimental study, *Contrib. Mineral. Petrol.*, *141*, 643–658.

Newton, R. C., T. V. Charlu, and O. J. Kleppa (1980), Thermochemistry of the high structural state plagioclases, *Geochim. Cosmochim. Acta*, *44*, 933–941.

Niu, F., A. Levander, C. M. Cooper, C.-T. A. Lee, A. Lenardic, and D. E. James (2004), Seismic constraints on the depth and composition of the mantle keel beneath the Kaapvaal craton, *Earth Planet. Sci. Lett.*, *224*, 337–346.

O'Connell, R. J., and B. Budiansky (1977), Viscoelastic properties of fluid saturated cracked solids, *J. Geophys. Res.*, *82*, 5719–5735.

Plafker, G., W. J. Nokleberg, and J. S. Lull (1989), Bedrock geology and tectonic evolution of the Wrangellia, Peninsular, and Chugach terranes along the Trans-Alaska Crustal Transect in the Chugach Mountains and southern Copper River Basin, Alaska, *J. Geophys. Res.*, *94*, 4255–4295.

Ringwood, A. E. (1979), Composition and origin of the Earth, in *The Earth: Its Origin, Structure and Evolution*, edited by M. W. McElhinny, pp. 1–54, Elsevier, New York.

Rudnick, R. L., and D. M. Fountain (1995), Nature and composition of the continental crust: A lower crustal perspective, *Rev. Geophys.*, *33*, 267–309.

Rudnick, R. L., and T. Presper (1990), Geochemistry of intermediate- to high-pressure granulites, in *Granulites and Crustal Evolution*, edited by D. Vielzeuf and P. Vidal, pp. 523–550, Springer, New York.

Saleeby, J., M. Ducea, and D. Clemens-Knott (2003), Production and loss of high-density batholithic root, southern Sierra Nevada, California, *Tectonics*, *22*(6), 1064, doi:10.1029/2002TC001374.

Schmeling, H. (1985), Numerical models on the influence of partial melt on elastic, anelastic, and electric properties of rocks. part I: Elasticity and anelasticity, *Phys. Earth Planet. Inter.*, *41*, 34–57.

Shaw, D. M., J. J. Cramer, M. D. Higgins, and M. G. Truscott (1986), Composition of the Canadian Precambrian shield and the continental crust of the Earth, in *The Nature of the Lower Continental Crust*, edited by J. B. Dawson, et al., *Geol. Soc. Spec. Publ.*, *24*, 275–282.

Shillington, D. J., H. J. A. Van Avendonk, W. S. Holbrook, P. B. Kelemen, and M. J. Hornbach (2004), Composition and structure of the central Aleutian island arc from arc-parallel wide-angle seismic data, *Geochem. Geophys. Geosyst.*, *5*, Q10006, doi:10.1029/2004GC000715.

Sobolev, S. V., and A. Y. Babeyko (1994), Modeling of mineralogical composition, density and elastic wave velocities in anhydrous magmatic rocks, *Surv. Geophys.*, *15*, 515–544.

Suyehiro, K., N. Takahashi, Y. Ariie, Y. Yokoi, R. Hino, M. Shinohara, T. Kanazawa, N. Hirata, H. Tokuyama, and A. Taira (1996), Continental crust, crustal underplating, and low-Q upper mantle beneath an oceanic island arc, *Science*, *272*, 390–392.

Tahirkheli, R. A. K. (1979), Geotectonic evolution of Kohistan, in *Geology of Kohistan, Karakoram Himalaya, Northern Pakistan. Geol. Bull.*, edited by R. A. K. Tahirkheli and M. Q. Jan, pp. 113–130, Univ. of Peshawar, Peshawar, Pakistan.

Taylor, S., and S. McLennan (1985), *The Continental Crust: Its Composition and Evolution*, Blackwell, Malden, Mass.

Taylor, S. R. (1967), The origin and growth of continents, *Tectonophysics*, *4*, 17–34.

Turcotte, D. L. (1989), Geophysical processes influencing the lower continental crust, in *Properties and Processes of Earth's Lower Crust*, *Geophys. Monogr. Ser.*, vol. 51, edited by R. F. Mereu, S. Mueller, and D. M. Fountain, pp. 321–329, AGU, Washington, D. C.

Wagner, L. S., S. Beck, and G. Zandt (2005), Upper mantle structure in the south central Chilean subduction zone (30° to 36°S), *J. Geophys. Res.*, *110*, B01308, doi:10.1029/2004JB003238.

Wagner, L. S., S. Beck, G. Zandt, and M. N. Ducea (2006), Depleted lithosphere, cold trapped asthenosphere, and frozen melt puddles above the flat slab in central Chile and Argentina, *Earth Planet. Sci. Lett.*, *245*, 289–301.

Watt, J. P., G. F. Davies, and R. J. O'Connell (1976), The elastic properties of composite materials, *Rev. Geophys.*, *14*, 541–563.

Weaver, B. L., and J. Tarney (1984), Empirical approach to estimating the composition of the continental crust, *Nature*, *210*, 575–577.

Wedepohl, K. H. (1994), The composition of the continental crust, *Mineral. Mag.*, *58*, 959–960.

Wei, C. J., and R. Powell (2003), Phase relations in high-pressure metapelities in the system KFMASH (K_2O-FeO-MgO-Al_2O_3-SiO_2-H_2O) with application to natural rocks, *Contrib. Mineral. Petrol.*, *145*, 301–315.

White, R. W., R. Powell, and T. J. B. Holland (2001), Calculation of partial melting equilibria in the system Na_2O-CaO-K_2O-FeO-MgO-Al_2O_3-SiO_2-H_2O (NCKFMASH), *J. Metamorph. Geol.*, *19*, 139–153.

White, R. W., R. Powell, and G. N. Phillips (2003), A mineral equilibria study of the hydrothermal alteration in mafic greenschist facies rocks at Kalgoorlie, Western Australia, *J. Metamorph. Geol.*, *21*, 455–468.

Wood, B. J., L. T. Bryndzia, and K. R. Johnson (1990), Mantle oxidation state and its relationship to tectonic environment and fluid speciation, *Science*, *248*, 337–345.

Zandt, G., H. Gilbert, T. Owens, M. Ducea, J. Saleeby, and C. Jones (2004), Active foundering of a continental arc root beneath the southern Sierra Nevada in California, *Nature*, *431*, 41–46.

M. D. Behn, Department of Geology and Geophysics, Woods Hole Oceanographic Institution, 360 Woods Hole Road, MS 22, Woods Hole, MA 02543, USA. (mbehn@whoi.edu)

P. B. Kelemen, Lamont-Doherty Earth Observatory, Columbia University, 58 Geochemistry Bldg., Palisades, NY 10964-0000, USA.